

# Optimal network topologies for information transmission in active networks

M. S. Baptista<sup>1</sup>, J. X. de Carvalho<sup>1</sup>, M. S. Hussein<sup>1,2</sup>

<sup>1</sup>*Max-Planck-Institut für Physik komplexer Systeme,  
Nöthnitzerstr. 38, D-01187 Dresden, Deutschland and*

<sup>2</sup>*Institute of Physics, University of São Paulo  
Rua do Matão, Travessa R, 187,  
05508-090, São Paulo - Brasil*

(Dated: November 8, 2018)

This work clarifies the relation between network circuit (topology) and behavior (information transmission and synchronization) in active networks, e.g. neural networks. As an application, we show how to determine a network topology that is optimal for information transmission. By optimal, we mean that the network is able to transmit a large amount of information, it possesses a large number of communication channels, and it is robust under large variations of the network coupling configuration. This theoretical approach is general and does not depend on the particular dynamic of the elements forming the network, since the network topology can be determined by finding a Laplacian matrix (the matrix that describes the connections and the coupling strengths among the elements) whose eigenvalues satisfy some special conditions. To illustrate our ideas and theoretical approaches, we use neural networks of electrically connected chaotic Hindmarsh-Rose neurons.

## I. AUTHOR SUMMARY

The relation between neural circuits and behavior is a fundamental matter in neuroscience. In this work, we present a theoretical approach that has the potential to unravel such a relationship in terms of network topology, information, and synchronization, in active networks, networks formed by elements that are dynamical systems (such as neurons, chaotic or periodic oscillators). As a direct application of our approaches, we show how one can construct optimal neural networks that not only transmit large amounts of information from one element to another in the network, but also are robust under alterations in the coupling configuration. We also show that the relation between synchronization and information is rather subtle. Neural networks whose configurations allow the transmission of large amounts of information might have at least two unstable modes of oscillation that are out of synchrony, while all the others are synchronous. Depending on the kind of measurement being done, one can arrive at contradicting statements concerning the relation between information and synchronization. We illustrate our theoretical approaches by using neural networks of electrically connected chaotic Hindmarsh-Rose neurons [1]. These results have a tremendous impact in the understanding of information transmission in brain-like networks, as well as, in the mammalian brain. They also shed light on a better understanding of the neural code, the rules under which neurons encode and transmit information about external stimuli.

## II. BLURB

This work shows how to relate in an active network the rate of information that can be transmitted from one point to another, regarded as mutual information rate (MIR), the synchronization level among elements, and

the connecting topology of the network.

## III. INTRODUCTION

Given an arbitrary time dependent stimulus that externally excites an active network formed by systems that have some intrinsic dynamics (e.g. neurons and oscillators), how much information from such stimulus can be realized by measuring the time evolution of one of the elements of the network ? Determining how and how much information flows along anatomical brain paths is an important requirement for the understanding of how animals perceive their environment, learn and behave [2, 3, 4].

The works of Refs. [2, 3, 4, 5, 6, 7] propose ways to quantify how and how much information from a stimulus is transmitted in neural networks. In particular, Ref. [5] demonstrated that 50% of the information about light displacements might be lost after being processed by the H1 neuron, sensitive to image motion around a vertical axis, a neuron localized in a small neural network of the *Chrysomya magacephala* fly, the lobula plate. Does that mean that the H1 neuron has an information capacity lower than the information contained in the light stimulus ? Or does that mean that information is lost due to the presence of internal noise ? These questions and others, which are still awaiting answers, concern the rules under which information is coded and then transmitted by neurons and it is a major topic of research in neuroscience referred to as the neural code [3, 4].

Even though the approaches of Ref. [2, 3, 4, 5, 6, 7] have brought considerable understanding on how and how much information from a stimulus is transmitted in a neural network, the relation between network circuits (topology) and information transmission in a neural as well as an active network is still awaiting a more quantitative description [8]. And that is the main thrust of

the present manuscript, namely, to present a quantitative way to relate network topology with information in active networks. Since information might not always be easy to be measured or quantified in experiments, we endeavour to clarify the relation between information and synchronization, a phenomenon which is often not only possible to observe but also relatively easy to characterize.

We initially proceed along the same line as in Refs. [9, 10], and study the information transfer in autonomous systems. However, instead of treating the information transfer between dynamical systems components, we treat the transfer of information per unit time exchanged between two elements in an autonomous chaotic active network. Thus, we neglect the complex relation between external stimulus and the network and show how to calculate an upper bound value for the mutual information rate (MIR) exchanged between two elements (a communication channel) in an autonomous network. Ultimately, we discuss how to extend this formula to non-chaotic networks suffering the influence of a time-dependent stimulus.

Most of this work is directed to ensure the plausibility and validity of the proposed formula for the upper bound of MIR (Sec. V) and also to study its applications in order to clarify the relation among network topology, information, and synchronization. We do not rely only on results provided by this formula, but we also calculate the MIR by the methods in Refs. [11, 12] and by symbolic encoding the trajectory of the elements forming the network and then measuring the mutual information provided by this discrete sequence of symbols (method described in Sec. XIII).

To illustrate the power of the proposed formula, we applied it to study the exchange of information in networks of coupled chaotic maps (Sec. XVI) and in Hindmarsh-Rose neural networks bidirectionally electrically coupled (Sec. VI). The analyses are carried out using quantities that we believe to be relevant to the treatment of information transmission in active networks: a *communication channel*, the *channel capacity*, and the *network capacity* (see definitions in Sec. XV).

A communication channel represents a pathway through which information is exchanged. In this work, a communication channel is considered to be formed by a pair of elements. One element represents a transmitter and the other a receiver, where the information about the transmitter can be measured.

The channel capacity is defined in terms of the proposed upper bound for the MIR. It measures the local maximal rate of information that two elements in a given network are able to exchange, a point-to-point measure of information exchange. As we shall see, there are two network configurations for which the value of the upper bound can be considered to be maximal with respect to the coupling strength.

The network capacity is the maximum of the KS-entropy, for many possible network configurations with a given number of elements. It gives the amount of in-

dependent information that can be simultaneously transmitted within the whole network, and naturally bounds the value of the MIR in the channels, which concerns only the transmission of information between two elements.

While the channel capacity is bounded and does not depend on the number of elements forming the network, the network capacity depends on the number of elements forming the network.

As a direct application of the formula for the upper bound value of the MIR, we show that an active network can operate with a large amount of MIR and KS-entropy and at the same time it is robustly resistant to alterations in the coupling strengths, if the eigenvalues of the Laplacian matrix satisfy some specified conditions (Sec. VII). The Laplacian matrix describes the connections among the elements of the network.

The conditions on the eigenvalues depend on whether the network is constructed in order to possess communication channels that are either self-excitable or non-self-excitable (see definition in Sec. XIV). Active networks that possess non-self-excitable channels (formed by oscillators as the Rössler, or the Chua's circuit) have channels that achieve their capacity whenever their elements are in complete synchrony. Therefore, if a large amount of information is desired to be transmitted point-to-point in a non-self-excitable network, easily synchronizable networks are required. On the other hand, networks that possess self-excitable channels (as the ones formed by neurons), achieve simultaneously its channel and network capacities when there is at least one unstable mode of oscillation (time-scale) that is out of synchrony (see Sec. XVII).

While non-self-excitable channels permit the exchanging of a moderate amount of information in a reliable fashion, due to the low level of desynchronization in the channel, self-excitable channels permit the exchange of surprisingly large amounts of information, not necessary reliable, due to the higher level of desynchronization in the channel.

In aiming at finding optimal network topologies, networks that can not only transmit large amounts of information but are also robust under alterations in the coupling strengths, we arrive at two relevant eigenvalues conditions which provide networks that satisfy all the optimal requirements. Either the network has elements that remain completely desynchronous for large variations of the coupling strength, forming the self-excitable channels, or the network has elements almost completely synchronous, forming the non-self-excitable channels. In fact, the studied network, a network formed by electrically connected Hindmarsh-Rose neurons, can have simultaneously self-excitable and non-self-excitable channels.

Self-excitable networks, namely those that have a majority number of self-excitable channels, have the topology of a perturbed star, i.e., they are composed of a central neuron connected to most of the other outer neurons, and some outer neurons sparsely connected among them-

selves. The networks that have non-self-excitable channels have the topology of a perturbed fully connected network, i.e., a network whose elements are almost all-to-all connected. The self-excitable network has thus a topology which can be considered to be a model for minicolumnar structure of the mammalian neocortex [13].

In order to construct optimal networks, we have used two approaches. Firstly, (Sec. VIII A), we use a Monte Carlo evolution technique [14] to find the topology of the network, assuming equal bidirectional coupling strengths. This evolving technique simulates the rewiring of a neuron network that maximizes or minimizes some cost function, in this case a cost function which produces optimal networks to transmit information. In the second approach (Sec. VIII B), we allow the elements to be connected with different coupling strengths. We then use the Spectral Theorem to calculate the coupling strengths of an all-to-all topology network.

Finally, we discuss how to extend these results to networks formed by elements that are non-chaotic (Sec. IX), and to non-autonomous networks, that are being perturbed by some time-dependent stimuli (Secs. IX and X).

## IV. RESULTS

### V. UPPER BOUND FOR THE MUTUAL INFORMATION RATE (MIR) IN AN ACTIVE NETWORK

In a recent publication [11], we have argued that the mutual information rate (MIR) between two elements in an active chaotic network, namely, the amount of information per unit time that can be realized in one element,  $k$ , by measuring another element,  $l$ , regarded as  $I_C$ , is given by the sum of the conditional Lyapunov exponents associated with the synchronization manifold (regarded as  $\lambda^{\parallel}$ ) minus the positive conditional Lyapunov exponents associated with the transversal manifold (regarded as  $\lambda^{\perp}$ ). So,  $I_C = \lambda^{\parallel} - \lambda^{\perp}$ .

As shown in [12], if one has  $N=2$  coupled chaotic systems, which produce at most two positive Lyapunov exponents  $\lambda_1, \lambda_2$  with  $\lambda_1 > \lambda_2$ , then  $\lambda^{\parallel} = \lambda_1$  and  $\lambda^{\perp} = \lambda_2$ . Denote the trajectory of the element  $k$  in the network by  $\mathbf{x}_k$ . For larger number of elements,  $N$ , the approaches proposed in [11] remain valid whenever the coordinate transformation  $\mathbf{X}_{k\parallel} = \mathbf{x}_k + \mathbf{x}_1$  (which defines the synchronization manifold) and  $\mathbf{X}_{k\perp} = \mathbf{x}_k - \mathbf{x}_1$  (which defines the transversal manifold) successfully separates the two systems  $k$  and  $l$  from the whole network. Such a situation arises in networks of chaotic maps of the interval connected by a diffusively (also known as electrically or linear) all-to-all topology, where every element is connected to all the other elements. These approaches were also shown to be approximately valid for chaotic networks of oscillators connected by a diffusively all-to-all topology. The purpose of the present work is to extend these

approaches and ideas to active networks with arbitrary topologies.

Consider an active network formed by  $N$  equal elements,  $\mathbf{x}_i$  ( $i = 1, \dots, N$ ), where every  $D$ -dimensional element has a different set of initial conditions, i.e.,  $\mathbf{x}_1 \neq \mathbf{x}_2 \neq \dots \neq \mathbf{x}_N$ . The network is described by

$$\dot{\mathbf{x}}_i = \mathbf{F}(\mathbf{x}_i) - \sigma \sum_j \mathcal{G}_{ij} \mathbf{H}(\mathbf{x}_j), \quad (1)$$

where  $\mathcal{G}_{ij}$  is the  $ij$  element of the coupling matrix. Since we choose  $\sum_j \mathcal{G}_{ij} = 0$  in order for a synchronization manifold to exist by the subspace  $\eta = \mathbf{x}_1 = \mathbf{x}_2 = \mathbf{x}_3 = \dots = \mathbf{x}_N$ , we can call this matrix the Laplacian matrix. The synchronous solution,  $\eta$ , is described by

$$\dot{\eta} = F(\eta) \quad (2)$$

The way small perturbations propagate in the network [17] is described by the  $i$  ( $i = 1, \dots, N$ ) variational equations of Eqs. (1), namely writing  $\mathbf{x}_i = \eta + \delta\mathbf{x}_i$  and expanding Eq. (1) in  $\delta\mathbf{x}_i$ ,

$$\delta\dot{\mathbf{x}}_i = [\nabla\mathbf{F}(\mathbf{x}_i) - \sigma \sum_{j=1}^N \mathcal{G}_{ij} D\mathbf{H}(\mathbf{x}_i)] \delta\mathbf{x}_i \quad (3)$$

obtained by linearly expanding Eq. (1). The spectra of Lyapunov exponent is obtained from Eq. (3).

Making  $\mathbf{x}_i = \xi$ , which can be easily numerically done by setting the elements with equal initial conditions and taking  $\mathbf{H}(\mathbf{x}_i) = \mathbf{x}_i$ , Eq. (3) can be made block diagonal resulting in

$$\dot{\xi}_i = [\nabla\mathbf{F}(\mathbf{x}_i) - \sigma\gamma_i] \xi_i. \quad (4)$$

where  $\gamma_i$  are the eigenvalues (positive defined) of the Laplacian matrix ordered such that  $\gamma_{i+1} \geq \gamma_i$ . Note that  $\gamma_1 = 0$ .

Notice that the network dynamics is described by Eq. (1), which assumes that every element has different initial conditions and therefore different trajectories (except when the elements are completely synchronized). On the other hand, Eq. (4) that provides the conditional exponents considers that all the initial conditions are equal. The equations for  $\xi_1$  describe the propagation of perturbations on the synchronization manifold  $\xi$ , and the other equations describe propagation of perturbations on the manifolds transversal to the synchronization manifold. While Eq. (3) provides the set of Lyapunov exponents of an attractor, Eq. (4) provides the Lyapunov exponents of the synchronization manifold and its transversal directions.

Notice also that when dealing with linear dynamics, the Lyapunov exponents [obtained from Eq. (3)] are equal to the conditional exponents [obtained from Eq. (4)] independently on the initial conditions.

Then, the upper bound of the MIR that can be measured from an element  $\mathbf{x}_k$  by observing another element

$\mathbf{x}_1$ , i.e. the upper bound of the MIR in the communication channel  $c^{i-1}$  is

$$I_P^{i-1} \leq |\lambda^1 - \lambda^i| \quad (5)$$

with  $i \in (2, \dots, N)$ , and  $\lambda^i$  representing the sum of all the **positive** Lyapunov exponents of the equation for the mode  $\xi_i$ , in Eq. (4). So,  $\lambda^1$  is the sum of the positive conditional exponents obtained from the separated variational equations, using the smallest eigenvalue associated with the exponential divergence between nearby trajectories around  $\xi$ , the synchronous state, and  $\lambda^i$  ( $i > 1$ ) are the sum of the positive conditional exponents of one of the possible desynchronous oscillation modes. Each eigenvalue  $\gamma_i$  produces a set of conditional exponents  $\lambda_m^i$ , with  $m = 1, \dots, D$ .

Each oscillatory mode  $\xi_i$  represents a subnetwork within the whole network which possesses some oscillatory pattern. This oscillatory subnetwork can be used for communications purposes. Each mode represents a path along which information can be transmitted through the network. The oscillation mode associated with the synchronization manifold ( $\xi_1$ ) propagates some information signal everywhere within the network. The desynchronous modes limits the amount of information that one can measure from the signal propagated by the synchronous mode. Although Eq. (5) gives the upper bound for the amount of information between modes of oscillation, for some simple network geometries, as the ones studied here, we can relate the amount of information exchanged between two vibrational modes to the amount of information between two elements of the network, and therefore, Eq. (5) can be used to calculate an upper bound for the MIR exchanged between pairs of elements in the network. For larger and complex networks, this association is non-trivial, and we rely on the reasonable argument that a pair of elements in an active network cannot transmit more information than some of the  $i - 1$  values of  $I_P^{i-1}$ .

The inequality in Eq. (5) can be interpreted in the following way. The right hand side of Eq. (5) calculates the amount of information that one could transmit if the whole network were completely synchronous with the state  $\xi$ , which is only true when complete synchronization takes place. Typically, we expect that the elements of the network will not be completely synchronous to  $\xi$ . While the positive conditional exponents associated with the synchronization manifold provide an upper bound for the rate of information to be transmitted, the transversal conditional exponents provide a lower bound for the rate of erroneously information exchanged between nodes of the network. Thus, the amount of information provided by the right part of Eq. (5) overestimates the exact MIR which, due to desynchronization in the network, should be smaller than the calculated one. For more details on the derivations of Eq. (5), see Sec. XVI.

Equation (6) allows one to calculate the MIR between oscillation modes of larger networks with arbitrary topology rescaling the MIR curve ( $I_P^1$  vs.  $\sigma$ ) obtained from two

coupled elements. Denoting  $\sigma^*(N = 2)$  as the strength value for which the curve for  $\lambda^2$  reaches a relevant value, say, its maximum value, then the coupling strength for which this same maximum is reached for  $\lambda^i$  in a network composed by  $N$  elements is given by

$$\sigma^{i*}(N) = \frac{2\sigma^*(N = 2)}{\gamma_i(N)} \quad (6)$$

where  $\gamma_i(N)$  represents the  $i$ th largest eigenvalue of the  $N$ -elements network. If the network has an all-to-all topology, thus,  $\sigma^*(N = 2)$  represents the strength value for which the curve of  $I_P^1$  reaches a relevant value, and  $\sigma^*(N)$  the strength value that this same value for  $I_P^i$  is reached.

Notice that symmetries in the connecting network topology leads to the presence of degenerate eigenvalues (=equal eigenvalues) in the Laplacian matrix, which means that there are less independent channels of communication along which information flows. Calling  $Q$  the number of degenerate eigenvalues of the Laplacian matrix, Eq. (5) will provide  $N - Q$  different values.

As the coupling strength  $\sigma$  is varied, the quantities that measure information change correspondingly. For practical reasons, it is important that we can link the way these quantities (see Sec. XV) change with the way the different types of synchronization show up in the network (see Sec. XVII). In short, there are three main types of synchronization observed in our examples: burst phase synchronization (BPS), when at least one pair of neurons are synchronous in the slow time-scale but desynchronous in the fast time-scale, phase synchronization (PS), when all pairs of neurons are phase synchronous, and complete synchronization (CS), when all pairs of neurons are completely synchronous. The coupling strength for which these synchronous phenomena appear are denoted by  $\sigma_{BPS}$ ,  $\sigma_{PS}$ , and  $\sigma_{CS}$  (with no superscript index).

Finally, there are a few more relevant coupling strengths, which characterize each communication channel. First,  $\sigma_{min}^i$ , for which the sum of the  $i$ th conditional exponents  $\lambda^i$  equals the value of  $\lambda^1$ . For  $\sigma < \sigma_{min}^i$ , the communication channel  $i$  (whose upper rate of information transmission depends on the two oscillation modes  $\xi_1$  and  $\xi_i$ ) behaves in a self-excitable way, i.e.,  $\lambda^1 < \lambda^i$ . For  $\sigma \geq \sigma_{min}^i$ ,  $\lambda^1 \geq \lambda^i$ . Secondly,  $\sigma^{i*}$  indicates the coupling strength at which  $I_P^{i-1}$  is maximal. Thirdly,  $\sigma_{CS}^i$  indicates the coupling strength for which the communication channel  $c^{i-1}$  becomes "stable", i.e.,  $\lambda^i < 0$ . At  $\sigma = \sigma^{i*}$  the self-excitable channel capacity of the channel  $c^{i-1}$  is reached and at  $\sigma = \sigma_{CS}^i$ , the non-self-excitable channel capacity is reached. Finally,  $\sigma_C$  is the coupling for which the network capacity is reached, and then, when the KS-entropy of the network is maximal. For other quantities, see Sec. XV.

## VI. THE MIR IN NETWORKS OF COUPLED HINDMARSH-ROSE NEURONS

We investigate how information is transmitted in self-excitable networks composed of  $N$  bidirectionally coupled Hindmarsh-Rose neurons [1]:

$$\begin{aligned}\dot{x}_i &= y_i + 3x_i^2 - x_i^3 - z_i + I_i + \sigma \sum_j \mathcal{G}_{ij}(x_j) \\ \dot{y}_i &= 1 - 5x_i^2 - y_i \\ \dot{z}_i &= -rz_i + 4r(x_i + 1.6)\end{aligned}\quad (7)$$

The parameter  $r$  modulates the slow dynamics and is set equal to 0.005, such that each neuron is chaotic. The index  $i \neq j$  assumes values within the set  $[1, \dots, N]$ .  $S_k$  represents the subsystem formed by the variables  $(x_k, y_k, z_k)$  and  $S_l$  represents the subsystem formed by the variables  $(x_l, y_l, z_l)$ , where  $k=[1, \dots, N-1]$  and  $l=[k+1, \dots, N]$ . The Laplacian matrix is symmetric, so  $\mathcal{G}_{ji} = \mathcal{G}_{ij}$ , and  $\sigma\mathcal{G}_{ji}$  is the strength of the electrical coupling between the neurons, and we take for  $I_i$  the value  $I_i = 3.25$ .

In order to simulate the neuron network and to calculate the Lyapunov exponents through Eq. (3), we use the initial conditions  $x=-1.3078+\eta$ ,  $y=-7.3218+\eta$ , and  $z=3.3530+\eta$ , where  $\eta$  is a uniform random number within  $[0, 0.02]$ . To calculate the conditional Lyapunov exponents, we use the equal initial conditions,  $x=-1.3078$ ,  $y=-7.3218$ , and  $z=3.3530$ .

**All-to-all coupling:** Here, we analyze the case where  $N$  neurons are fully connected to every other neuron. The Laplacian matrix has  $N$  eigenvalues,  $\gamma_1=0$ , and  $N-1$  degenerate ones  $\gamma_i=N$ ,  $i=2, \dots, N$ . Every pair of neurons exchange an equal amount of MIR. Although, there are  $N \times (N-1)/2$  pairs of neurons, there is actually only one independent channel of communication, i.e., a perturbation applied at some point of the network should be equally propagated to all other points in the network. In Fig. 1(A), we show the MIR,  $I_C$ , calculated using the approaches in Refs. [11, 12],  $I_P$ , calculated using the right hand-side of Eq. (5), and  $I_S$ , calculated encoding the trajectory between pair of neurons (Sec. XIII), and the Kolmogorov-Sinai entropy,  $H_{KS}$ , for a network composed by  $N=2$  neurons. In (B), we show these same quantities for a network formed by  $N=4$  neurons.

While for  $\sigma \cong 0$  and  $\sigma \geq \sigma_{CS}$ , we have that  $I_C \cong I_P \cong I_S$ , for  $\sigma \cong \sigma^{2*}$  (when the self-excitable channel capacity is reached) it is clear that  $I_P$  should be an upper bound for the MIR, since not only  $I_P > I_C$  but also  $I_P > I_S$ . Notice the good agreement between  $I_C$  and  $I_S$ , except for  $\sigma \cong \sigma_{min}^2$ , when  $I_S > H_{KS}$ , which violates Eq. (13).

The star symbol indicates the value of the coupling,  $\sigma_{BPS}$  (Sec. XVII), for which burst phase synchronization (BPS) appears while the spikes are highly desynchronous. The appearance of BPS coincides with the moment where all the quantifiers for the MIR are large, and close to a coupling strength,  $\sigma_C$ , for which the network capacity is reached (when  $H_{KS}$  is maximal).

At this point, the network is sufficiently desynchronous to generate a large amount of entropy, which implies a large  $\lambda^i$ , for  $i \geq 2$ . This is an optimal configuration for the maximization of the MIR. There exists phase synchrony in the subspace of the slow time-scale  $z$  variables (which is responsible for the bursting-spiking behavior), but there is no synchrony in the  $(x, y)$  subspace. This supports the binding hypothesis, a fundamental concept of neurobiology [13] which sustains that neural networks coding the same feature or object are functionally bounded. It also simultaneously supports the works of [15], which show that desynchronization seems to play an important role in the perception of objects as well. Whenever  $\lambda^2$  approaches zero, at  $\sigma = \sigma_{CS}$ , there is a drastic reduction in the value of  $H_{KS}$  as well as  $I_P$ , since the network is in complete synchronization (CS), when all the variables of one neuron equals the variables of the other neurons.

Therefore, for coupling strengths larger than the one indicated by the star symbol, and smaller than the one where CS takes place, there is still one time-scale, the fast time-scale, which is out of synchrony.

For  $\sigma > \sigma_{min}^2$ , the only independent communication channel is of the non-self-excitable type. That means  $\lambda^i \leq \lambda^1$  ( $i \geq 2$ ), and as the coupling strength increases,  $H_{KS}$  decreases and  $I_P$  increases.

Note that the curve for  $I_P$  shown in Fig. 1(B) can be obtained by rescaling the curve shown in Fig. 1(A), applying Eq. (6).

**Nearest-neighbor coupling:** Here, every neuron is connected to its nearest neighbors, with periodic boundary conditions, forming a closed ring. The eigenvalues of the Laplacian matrix can be calculated from  $\gamma_k = 4 \sin\left(\frac{\pi(k-1)}{N}\right)^2$ ,  $k \in [1, \dots, N]$ . Notice that in this example,  $\gamma_{k+1}$  might be smaller than  $\gamma_k$  due to the degeneracies. We organize the eigenvalues in a crescent order. For our further examples, we consider  $N=4$  [in Fig. 2(A)] and  $N=6$  [in Fig. 2(B)]. For  $N=4$ ,  $\gamma_1=0$ ,  $\gamma_{2,3}=2$ ,  $\gamma_4=4$ , and for  $N=6$ ,  $\gamma_1=0$ ,  $\gamma_{2,3}=1$ ,  $\gamma_{4,5}=3$ ,  $\gamma_6=4$ .

Networks with a nearest-neighbor coupling topology and an even number of elements possess a connecting matrix  $\mathcal{G}$  with  $N/2-1$  degenerate eigenvalues, and therefore,  $N-N/2+1$  distinct eigenvalues. There are only  $N-N/2$  different minimal path lengths connecting the elements of the network. The minimal path length quantifies the minimal distance between an element and another in the network by following a path formed by connected elements. Note that  $I_P$  assumes only  $N-N/2$  different values. It is reasonable to state that each different value corresponds to the exchange of information between elements that have the same minimal path length.

For a network with  $N=4$  [Fig. 2(A)], there are two possible minimal path lengths, 1 and 2. Either the elements are 1 connection apart, or 2 connections apart. For such a network, it is reasonable to associate  $I_P^1 = \lambda^1 - \lambda^2$  with the MIR between two elements,  $S_k$  and  $S_{k+2}$ , that are 2 connections apart, and  $I_P^3 = |\lambda^1 - \lambda^4|$  to the MIR between two elements,  $S_k$  and  $S_{k+1}$ , that are 1 connection

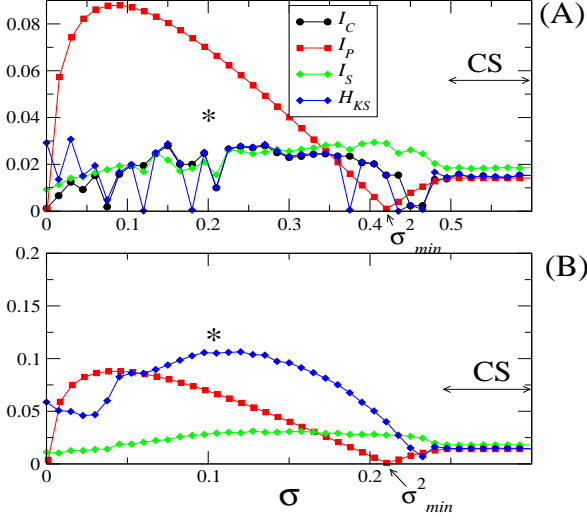


FIG. 1: The quantities  $I_C$  (black circles),  $I_P$  (red squares),  $I_S$  (green diamonds), and  $H_{KS}$  (blue diamonds), for two (A) and four (B) coupled neurons, in an all-to-all topology. Notice that since there are only two different eigenvalues, there is only one channel of communication whose upper bound for the MIR is given by  $I_P = |\lambda^1 - \lambda^2|$ . Also,  $I_S$  and  $I_C$  represent the mutual information exchanged between any two pairs of elements in the system. In (A),  $\sigma^{2*} = 0.092$ ,  $\sigma_{BPS} \cong 0.2$ ,  $\sigma_{min}^2 = 0.42$ ,  $\sigma_{PS} = 0.47$ , and  $\sigma_{CS} = 0.5$ . In (B),  $\sigma^{2*} = 0.046$ ,  $\sigma_{BPS} \cong 0.1$ ,  $\sigma_{min}^2 = 0.21$ ,  $\sigma_{PS} = 0.24$ , and  $\sigma_{CS} = 0.25$ . CS indicates the coupling interval  $\sigma \geq \sigma_{CS}$  for which there exists complete synchronization.

apart. The more distant (closer) an element is from any other, the larger (smaller) the coupling strength for them to synchronize. In addition,  $\sigma^{2*} > \sigma^{4*}$  and  $\sigma_{min}^2 > \sigma_{min}^4$ . That means that the more distant elements are from each other the larger the coupling strength is, in order for these two elements to exchange a large rate of information, since  $\sigma^{2*} > \sigma^{4*}$ . In addition, since  $\sigma_{min}^2 > \sigma_{min}^4$ , the communication channel responsible for the exchange of information between closer elements (the channel  $c^3$ ) becomes non-self-excitable for a smaller value of the coupling strength than the strength necessary to turn the communication channel responsible for the exchange of information between distant elements (the channel  $c^1$ ) into a non-self-excitable channel. Since the level of desynchronization in a non-self-excitable channel is low, then, closer elements can exchange reliable information for smaller coupling strengths than the strength necessary for distant elements to exchange reliable information. Note that due to the 1 degenerated eigenvalue,  $I_P^1 = I_P^2$ ,  $\sigma^{2*} = \sigma^{3*}$ , and  $\sigma_{min}^2 = \sigma_{min}^3$ . A similar analysis can be done for the network  $N=6$ , whose results are shown in Fig. 2(B).

The KS entropy of the network,  $H_{KS}$ , is also shown in this figure. In (A),  $\sigma_{min}^2 = 0.42$  and  $\sigma_{min}^4 = 0.21$ , and

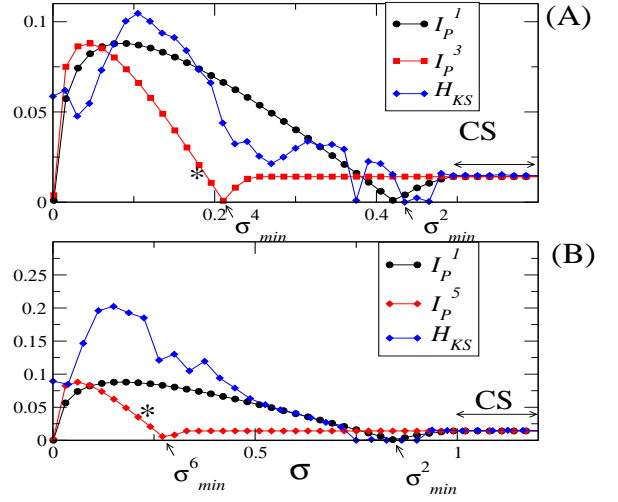


FIG. 2: The quantities  $I_P$  and  $H_{KS}$  for nearest-neighbor networks with  $N=4$  (A) and  $N=6$  (B). In (A),  $\sigma^{2*} = 0.09$ ,  $\sigma^{4*} = 0.046$ ,  $\sigma_{min}^2 = 0.42$ ,  $\sigma_{min}^4 = 0.21$ ,  $\sigma_{CS}^4 = 0.25$ ,  $\sigma_{BPS} \cong 0.18$ ,  $\sigma_{PS} = 0.462$ , and  $\sigma_{CS} = 0.5$ . In (B),  $\sigma^{2*} = 0.18$ ,  $\sigma^{6*} = 0.061$ ,  $\sigma_{min}^2 = 0.84$ ,  $\sigma_{min}^6 = 0.27$ ,  $\sigma_{CS}^6 = 0.33$ ,  $\sigma_{BPS} \cong 0.23$ ,  $\sigma_{PS} = 0.78$ , and  $\sigma_{CS} = 1.0$ . The stars point to where BPS first appears. CS indicates the coupling interval  $\sigma \geq \sigma_{CS}$  for which there exists complete synchronization.

in (B),  $\sigma_{min}^2 = 0.84$  and  $\sigma_{min}^6 = 0.275$ , values that can be easily derived from Eq. (6). Note that the values of  $\sigma = \sigma_{min}^4$  in (A) [and  $\sigma = \sigma_{min}^6$ , in (B)] are close to the parameter for which BPS in the slow time-scale is first observed in these networks (indicated by the star symbol in Fig. 2),  $\sigma_{BPS} \cong 0.18$  [in (A)] and  $\sigma_{BPS} \cong 0.23$  [in (B)]. At  $\sigma \cong \sigma_{min}^4$  [in (A)] and  $\sigma \cong \sigma_{min}^6$  [in (B)], also the quantities  $I_P^1$  and  $H_{KS}$  are large.

Another important point to be emphasized in these networks is that  $\Delta\sigma_{NSE}^i = \sigma_{CS} - \sigma_{min}^i$ , regarded as the non-self-excitable robustness parameter for the communication channels  $c^i$ , with  $i=3$  for the network with  $N=4$  [in (A)] and  $i=5$  for the network with  $N=6$  [in (B)] is large. This is a consequence of the fact that the normalized spectral distance (NED),  $(\gamma_i - \gamma_2)/N$  is also large, for either  $i=4$  [in (A)] or  $i=6$  [in (B)]. Having a large NED between the  $i$ th largest and the first largest eigenvalues results in a non-self-excitable channel,  $c^{i-1}$ , robust under large alterations of the coupling strength. On the other hand,  $\Delta\sigma_{SE}^i = \sigma_{min}^i$ , regarded as the self-excitable robustness parameter for the communication channel  $c^{i-1}$ , is large, for  $i=2, 3$ . This is a consequence of the fact that the normalized spectral distance (NED),  $(\gamma_N - \gamma_i)/N$  is large. Having a large NED between the largest and the  $i$ th largest eigenvalues results in a self-excitable channel,  $c^{i-1}$ , robust under large alterations of the coupling strength.

Notice also that the maximal values of  $I_P$  for the all-to-

all and nearest-neighbor networks topologies is the same (see Figs. 1 and 2). This shows that the maximum of  $I_P$  does not depend on the number,  $N$ , of elements in the network. Not so in the case of the network capacity  $\mathcal{C}_C$ , which increases with  $N$ . Thus, pairs of elements can transmit information in a rather limited rate, but depending on the number of elements forming the network, a large number of channels can simultaneously transmit information.

**Star coupling:** We consider  $N=4$ . There is a central neuron, denoted by  $S_1$ , bidirectionally connected to the other three ( $S_k, k = 2, 3, 4$ ), but none of the others are connected among themselves. The eigenvalues of the Laplacian matrix are  $\gamma_1=0, \gamma_{2,3}=1, \gamma_4 = N$ . So, not only the NED between  $\gamma_N$  and  $\gamma_{N-1}$  is large but also between  $\gamma_N$  and  $\gamma_{N-2}$ , and therefore,  $\Delta\sigma_{SE}^{N-1}$  and  $\Delta\sigma_{SE}^{N-2}$  are large. This provides a network whose channels  $c^1$  and  $c^2$  have a large MIR for a large coupling strength alteration. Note that if  $\gamma_{N-1}$  is far away from  $\gamma_N$  that implies that  $\gamma_{N-2}$  is also far away from  $\gamma_N$ . Thus, a reasonable spectral distance between  $\gamma_{N-1}$  and  $\gamma_N$  is a “biological requirement” for the proper function of the network, since even for larger coupling strengths there will be at least one oscillation mode which is desynchronous, a configuration that enables perturbation (meaning external stimuli) to be propagated within the network [16].

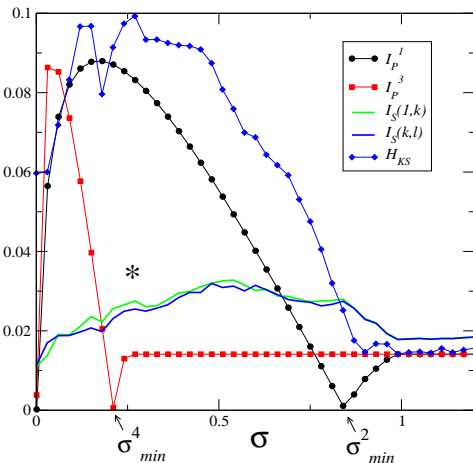


FIG. 3: MIR between the central neuron and an outer one (black circles),  $I_P^1$ , (resp.  $I_S(1, k)$ , in green line), and between two outer ones (red squares),  $I_P^3$ , (resp.  $I_S(k, l)$ , in blue line). Blue diamonds represents the KS-entropy. Other quantities are  $\sigma^{4*} = 0.181$ ,  $\sigma^{2*} = 0.044$ ,  $\sigma_{min}^4 = 0.84$ ,  $\sigma_{min}^2 = 0.22$ ,  $\sigma_{CS}^4 = 0.27$ ,  $\sigma_{BPS} = 0.265$ ,  $\sigma_{PS} = 0.92$ , and  $\sigma_{CS} = 1.0$ . The star indicates the parameter for which BPS first appears.

The largest eigenvalue is related to an oscillation mode where all the outer neurons are in synchrony with each other but desynchronous with the central neuron. So,

here it is clear the association between  $|\lambda^1 - \lambda^4|$  and the MIR between the central neuron with an outer neuron, since  $\lambda^1$  represents the amount of information of the synchronous trajectories among all the neurons, while  $\lambda^4$  is the amount of information of the desynchronous trajectories between the central neuron and any outer neuron. The other eigenvalues ( $\gamma_2, \gamma_3$ ) represent directions transverse to the synchronization manifold in which the outer neurons become desynchronous with the central neuron in waves wrapping commensurately around the central neuron [17]. Thus,  $\lambda^2$  and  $\lambda^3$  are related to the error in the transmission between two outer neurons,  $k$  and  $l$ , with  $k, l \neq 1$ .

Note that the MIR between  $S_1$  and an outer neuron (upper bound represented by  $I_P^3 = |\lambda^1 - \lambda^4|$  and  $I_S$  represented by  $I_S(1, k)$ , in Fig. 3) is larger (smaller) than the MIR between two outer neurons (upper bound represented by  $I_P^1 = |\lambda^1 - \lambda^2|$  and  $I_S$  is represented by  $I_S(k, l)$ , in Fig. 3), for small coupling (for when the channel  $c^3$  is self-excitable, and  $\sigma \geq \sigma_{min}^4$ ). Similar to the nearest-neighbor networks, the self-excitable and the non-self-excitable channel capacities of the channel associated with the transmission of information between closer elements (the channel  $c^3$ ) are achieved for a smaller value of the coupling strength than the one necessary to make the channels associated with the transmission of information between more distant elements (the channel  $c^1$ ) to achieve its two channel capacities. That property permits this network, for  $\sigma \cong \sigma_{min}^4$ , to transmit simultaneously reliable information using the channel  $c^3$  and with a higher rate using the channel  $c^1$ .

Notice, in Fig. 3, that  $\sigma^{2*} \cong \sigma_{min}^4 \cong \sigma_{BPS} \cong \sigma_C$ . So, when the channel capacity of the channel  $c^1$  is reached, also  $H_{KS}$  of the network is maximal, and the network operates with its capacity.

Another point that we want to emphasize in this network is that while a large NED between  $\gamma_N$  and  $\gamma_{N-1}$  provides a network whose channel  $c^1$  is self-excitable and can transmit information at a large rate for a large coupling strength interval, a large NED between  $\gamma_3$  and  $\gamma_2$  leads to a non-self-excitable channel  $c^3$  even for small values of the coupling amplitudes, and it remains non-self-excitable for a large variation of the coupling strength. Thus, while a large NED between the second and the first largest eigenvalues leads to a network whose channels are predominantly of the self-excitable types, a large NED between the second largest and the third largest eigenvalues provide a network whose communication channels are predominantly of the non-self-excitable types.

## VII. EIGENVALUES CONDITIONS FOR OPTIMAL NETWORK TOPOLOGIES

Finding network topologies and coupling strengths in order to have a network that operates in a desired fashion is not a trivial task (see Sec. XVIII and XIX). An ideal way to proceed would be to evolve the network topology

in order to achieve some desired behavior. In this paper, we are interested in maximizing simultaneously  $I_P$ , the KS-entropy, and the average  $\langle I_P \rangle$ , for a large range of the coupling strength, characteristics of an *optimal network*. However, evolving a network in order to find an optimal one would require the calculation of the MIR in every communication channel and  $H_{KS}$  for every evolution step. For a typical evolution, which requires  $10^6$  evolution steps, such an approach is impractical.

Based on our previous discussions, however, an optimal network topology can be realized by only selecting an appropriate set of eigenvalues which have some specific NED. Evolving a network by the methods of Secs. XVIII and XIX using a cost function which is a function of only the eigenvalues of the Laplacian matrix is a practical and physibly task.

The present section is dedicated to describe the derivation of this cost function.

We can think of two most relevant sets of eigenvalues which create optimal networks, and they are represented in Fig. 4. Either it is desired eigenvalues that produce a network predominantly self-excitable [SE, in Fig. 4] or predominantly non-self-excitable [NSE, in Fig. 4].

In a network whose communication channels are predominantly self-excitable, it is required that the NED  $(\gamma_N - \gamma_{N-1})/N$  is maximal and  $(\gamma_{N-1})/N$  minimal. Therefore, we want a network for which the cost function

$$\mathcal{B}_1 \equiv \frac{\gamma_N - \gamma_{N-1}}{\gamma_{N-1}} \quad (8)$$

is maximal.

A network whose eigenvalues maximize  $\mathcal{B}_1$  has self-excitable channels for a large variation of the coupling strength. As a consequence,  $\langle I_P \rangle$  as well as  $H_{KS}$  is large for  $\sigma \in [\sigma_{min}^N, \sigma_{min}^2]$ .

In a network whose communication channels are predominantly non-self-excitable, it is required that the NED  $(\gamma_3 - \gamma_2)/N$  is maximal and  $(\gamma_2)/N$  minimal. Therefore, we want a network for which the cost function

$$\mathcal{B}_2 \equiv \frac{\gamma_3 - \gamma_2}{\gamma_2} \quad (9)$$

is maximal.

A network whose eigenvalues maximize the condition in Eq. (9) have non-self-excitable channels for a large variation of the coupling strength. As a consequence,  $\langle I_P \rangle$  is large for  $\sigma \in [\sigma_{min}^N, \sigma_{min}^3]$ , which is a small coupling range, but since there is still one oscillation mode that is unstable (the mode  $\xi_2$ ),  $H_{KS}$  is still large for a large range of the coupling strength ( $\sigma < \sigma_{min}^2$ ). Most of the channels will transmit information in a reliable way, since the error in the transmission, provided by  $\lambda^i$  ( $i \geq 2$ ), of most of the channels will be zero, once  $\lambda^i < 0$ .

Since degenerate eigenvalues produce networks with less vibrational modes, we assume in the following the absence of such degenerate eigenvalues. In addition, we

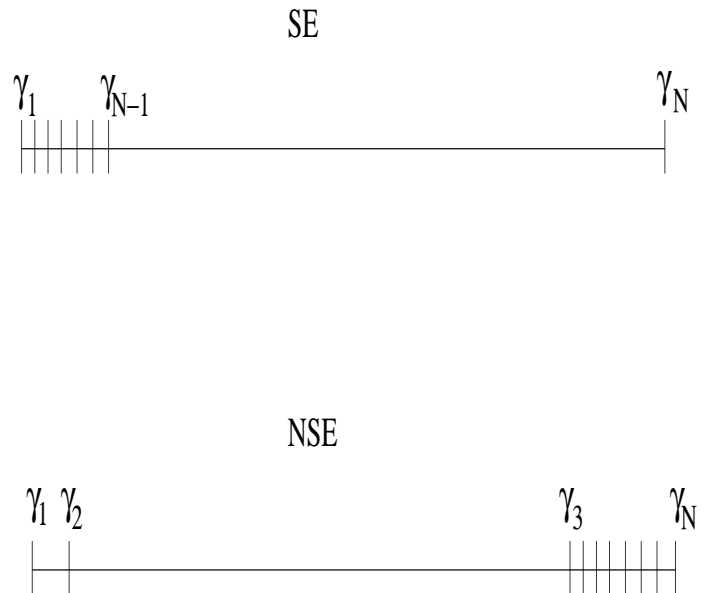


FIG. 4: Representation of the eigenvalues sets that produce optimal self-excitable (SE) and non-self-excitable active networks (NSE).

assume that there is a finite distance between eigenvalues so that the network becomes robust under rewiring, and therefore, perturbing  $\mathcal{G}_{ij}$  will not easily create degenerate eigenvalues.

A network that is completely synchronous and has no unstable modes does not provide an appropriate environment for the transmission of information about an external stimulus, because they prevent the propagation of perturbations. Networks that can be easily completely synchronized (for small coupling strengths) requires the minimization of  $\gamma_N - \gamma_2$ , or in terms of the eigenratio, the minimization of  $\gamma_N/\gamma_2$ . We are not interested in such a case. To construct network topologies that are good for complete synchronization, see Refs. [17, 18, 19].

## VIII. OPTIMAL TOPOLOGIES FOR INFORMATION TRANSMISSION

Before explaining how we obtain optimal network topologies for information transmission, it is important to discuss the type of topology expected to be found by maximizing either  $\mathcal{B}_1$ , in Eq. (8) or  $\mathcal{B}_2$ , in Eq. (9). Notice that Laplacians whose eigenvalues maximize  $\mathcal{B}_1$  are a perturbed version of the star topology, and the ones that maximize  $\mathcal{B}_2$  are a perturbed version of the all-to-all topology. In addition, in order to have a network that presents many independent modes of oscillations it is required that the Laplacian matrix presents as much as possible, a large number of non-degenerate eigenvalues. That can be arranged by rewiring (perturbing) networks possessing either the star or the nearest-neighbor topology, breaking the symmetry.



In order to calculate an optimal Laplacian, we propose two approaches.

One approach, described in Sec. XVIII, is based on the reconstruction of the network by evolving techniques, simulating the process responsible for the growing or rewiring of real biological networks, a process which tries to maximize or minimize some cost function. The results are discussed in Sec. VIII A.

A second approach, described in Sec. XIX, is based on the Spectral Theorem, and produces a network in order for its Laplacian to have a previously chosen set of eigenvalues. These eigenvalues can be chosen in order to maximize the cost function. The results are discussed in Sec. VIII B.

### A. Evolving networks

In order to better understand how a network evolves (grows) in accordance with the maximization of the cost functions in Eqs. (8) and (9), we first find the network configurations with a small number of elements. To be specific, we choose  $N=8$  elements. To show that indeed the calculated network topologies produce active networks that operate as desired, we calculate the average upper bound value of the MIR [Eq. (12)] for neural networks described by Eqs. (7) with the topology obtained by the evolution technique, and compare with other network topologies. Figure 5 shows  $\langle I_P \rangle$ , the average channel capacity, calculated for networks composed of 8 elements, using one of the many topologies obtained by evolving the network maximizing  $\mathcal{B}_1$  (circles, denoted in Fig. by "evolving 1"), all-to-all topology (squares), star topology (diamonds), nearest-neighbor (upper triangle), and maximizing  $\mathcal{B}_2$  (down triangle, denoted in Fig. by "evolving 2"). The star points to the value of  $\sigma_{min}^2$ , when  $c^1$ , the most unstable communication channel (a self-excitable channel), becomes non-self-excitable.

As desired the evolving network 1 has a large upper bound for the MIR (as measured by  $\langle I_P \rangle$ ) for a large range of the coupling strength, since the network has predominantly self-excitable channels. The channel  $c^1$  has a large robustness parameter  $\Delta\sigma_{SE}^2$ , i.e., it is a self-excitable channel for  $\sigma < \sigma_{min}^2$ , where  $\sigma_{min}^2=2.0$ . In contrast to the other topologies, in the star, nearest-neighbor, and all-to-all topologies,  $\Delta\sigma_{SE}^2$  is smaller and  $\Delta\sigma_{NSE}^2$  is larger. Even though most of the channels in the evolving 2 topology are of the non-self-excitable type,  $\langle I_P \rangle$  remains large even for higher values of the coupling strength. That is due to the channel  $c^1$  which turns into a self-excitable channel only for  $\sigma > 2$ .

The KS-entropies of the 5 active networks whose  $\langle I_P \rangle$  are shown in Fig. 5 are shown in Fig. 6. Typically, the network capacities are reached for roughly the same coupling strength for which the maximum of  $\langle I_P \rangle$ , is reached. In between the coupling strength for which the network capacities and the maximal of  $\langle I_P \rangle$  are reached,  $\lambda^3$  becomes negative. At this point, also BPS appears in the

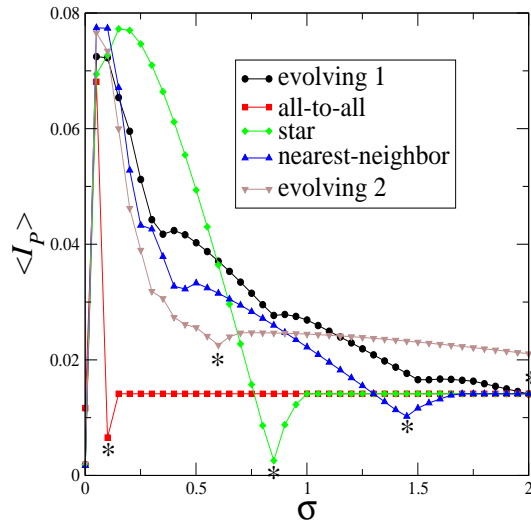


FIG. 5: The average value of the upper bound MIR,  $\langle I_P \rangle$  [as defined in Eq. (12)] for active networks composed of 8 elements using one of the many topologies obtained by evolving the network maximizing  $\mathcal{B}_1$  (circles), all-to-all topology (squares), star topology (diamonds), nearest-neighbor (upper triangle), and maximizing  $\mathcal{B}_2$  (down triangle). The values of  $\sigma_{min}^2$  indicated by the starts are  $\sigma_{min}^2=0.169$  (evolving 1),  $\sigma_{min}^2=0.05$  (all-to-all),  $\sigma_{min}^2=0.037$  (star),  $\sigma_{min}^2=0.037$  (nearest-neighbor), and  $\sigma_{min}^2=0.6$  (evolving 2). The evolving 1 network has a Laplacian with relevant eigenvalues  $\gamma_7=3.0000$ ,  $\gamma_8=6.1004$ , which produces a cost function equal to  $\mathcal{B}_1=1.033$ . The evolving 2 network has a Laplacian with relevant eigenvalues  $\gamma_2=0.2243$  and  $\gamma_3=1.4107$ , which produces a cost function equal to  $\mathcal{B}_2=5.2893$ .

slow time-scale, suggesting that this phenomena is the behavioral signature of a network that is able to transmit not only large amounts of information between pairs of elements (high MIR) but also overall within the network (high  $H_{KS}$ ).

Note however, that since the evolving networks have a small number of elements, the cost function cannot reach higher values and therefore, the networks are not as optimal as they can be. For that reason, we proceed now to evolve larger networks, with  $N=32$ .

Maximization of the cost function  $\mathcal{B}_1$  leads to the network connectivity shown in Fig. 7(A) and maximization of the cost function  $\mathcal{B}_2$  leads to the network connectivity shown in Fig. 7(B). In (A), the network has the topology of a perturbed star, a neuron connected to all the other outer neurons, thus a hub, and each outer neuron is sparsely connected to other outer neurons. The arrow points to the hub. In (B), the network has the topology of a perturbed all-to-all network, where elements are almost all-to-all connected. Note that there is one element, the neuron  $S_{32}$ , which is only connected to one neuron, the  $S_1$ . This isolated neuron is responsible to produce the large spectral gap between the eigenvalues  $\gamma_3$  and  $\gamma_2$ .

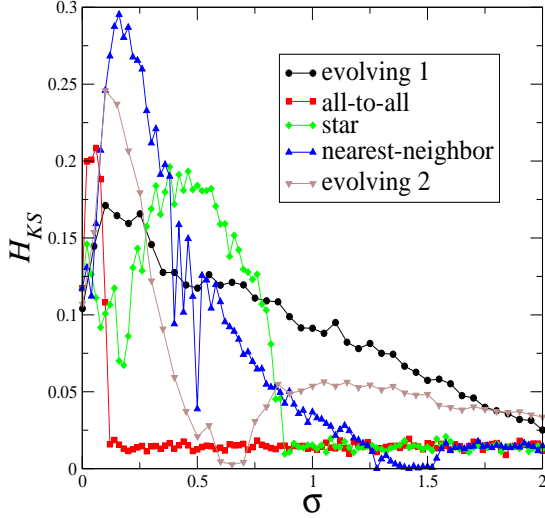


FIG. 6: KS-entropy for the same active networks of Fig. 5 composed of 8 elements.

$\langle I_P \rangle$  for the network topology represented in Fig. 7(A) is shown in Fig. 8 as circles, and  $\langle I_P \rangle$  for the network topology represented in Fig. 7(B) is shown in Fig. 8 as squares. We see that the star topology, whose connectivity is represented in 7(A), has larger  $\langle I_P \rangle$  for a larger coupling strength than the topology whose connectivity is represented in 7(B). Other relevant parameters of the network whose topology is represented in 7(A) are  $\sigma_{min}^2=0.8468$ ,  $\sigma_{min}^3=0.8249$ ,  $\sigma_{min}^N=0.0278$ ,  $\sigma_{CS}=0.9762$  and for the topology represented in 7(B) are  $\sigma_{min}^2=0.8512$ ,  $\sigma_{min}^3=0.042$ ,  $\sigma_{min}^N=0.031$ , and  $\sigma_{CS}=0.9761$ .

It is worth to comment that the neocortex is being simulated in the Blue Brain project, by roughly creating a large network composed of many small networks possessing the star topology. By doing that, one tries to recreate the way minicolumnar structures [13] are connected to minicolumnar structures of the neocortex [20]. Each minicolumn can be idealized as formed by a pyramidal neuron (the hub) connected to its interneurons, the outer neurons in the star topology, which are responsible for the connections among this minicolumn (small network) to others minicolumn. So, the used topology to simulate minicolumns is an optimal topology in what concerns the transmission of information.

### B. Constructing a network by a given set of eigenvalues

It is of general interest to assess if the eigenvalues obtained from the method in Sec. XVIII (in order to have a network Laplacian whose eigenvalues maximize the cost function  $\mathcal{B}$ ) can be used to construct other net-

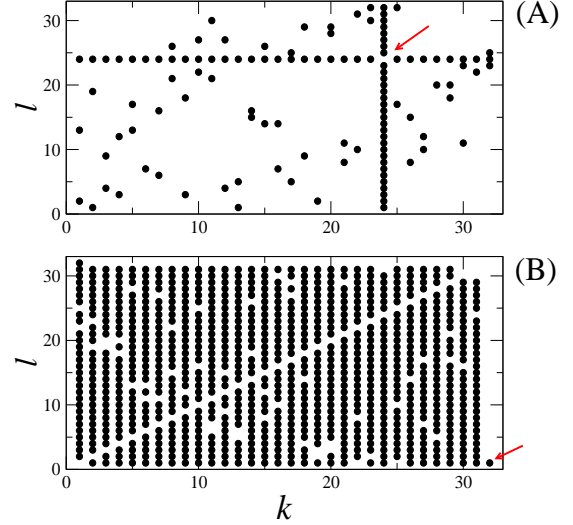


FIG. 7: A point in this figure in the coordinate  $k \times l$  means that the elements  $S_k$  and  $S_l$  are connected with equal couplings in a bidirectional fashion. In (A), a 32 elements network, constructed by maximizing the cost function  $\mathcal{B}_1$  in Eq. (8) and in (B), 32 elements network, constructed by maximizing the cost function  $\mathcal{B}_2$  in Eq. (9). In (A), the network has the topology of a perturbed star, a hub of neurons connected to all the other neurons, where each outer neuron is sparsely connected to other neurons. The arrow points to the hub. In (B), the network has the topology of a perturbed all-to-all network, where elements are almost all-to-all connected. Note that there is one element, the neuron  $S_{32}$ , which is only connected to one neuron, the  $S_1$ . This isolated neuron is responsible to produce the large spectral gap between the eigenvalues  $\gamma_3$  and  $\gamma_2$ . In (A), the relevant eigenvalues are  $\gamma_{31}=4.97272$ ,  $\gamma_{32}=32$ , which produce a cost function equal to  $\mathcal{B}=5.43478$ . In (B), the relevant eigenvalues are  $\gamma_2=0.99761$ ,  $\gamma_3=27.09788$ , which produce a cost function equal to  $\mathcal{B}_2=26.1628$ .

works (whose Laplacian preserve the eigenvalues) maintaining still the properties here considered to be vital for information transmission.

By a given set of eigenvalues, one can create a Laplacian matrix,  $\mathcal{G}'$ , with non-zero real entries, using the method described in Sec. XIX. The resulting network will preserve the eigenvalues and the synchronous solution in Eq. (2), which means that the values of  $I_P^i$  of the topology created by the method in Sec. XIX are equal to the values of the network topologies that provide the set of eigenvalues, in the following example, the network connectivities represented in Fig. 7(A-B).

In Fig. 9(A-B), circles represent the values of  $H_{KS}$  for the network whose connectivities are represented in Figs. 7(A-B), and the squares represent this same quantity for a network whose Laplacian is calculated by the method in Sec. XIX, in order to preserve the same eigenvalues of the network topologies represented in Fig. 7(A-B).

The main difference between these two networks is that for the one constructed by the method in Sec. XIX, when

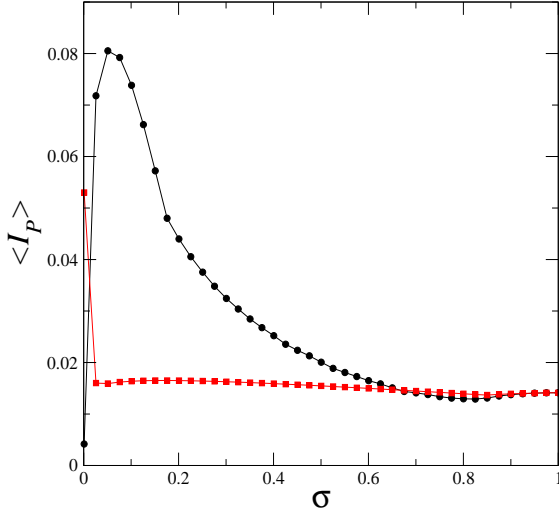


FIG. 8:  $\langle I_P \rangle$  for the networks shown in Fig. 7(A-B) by circles and squares, respectively.

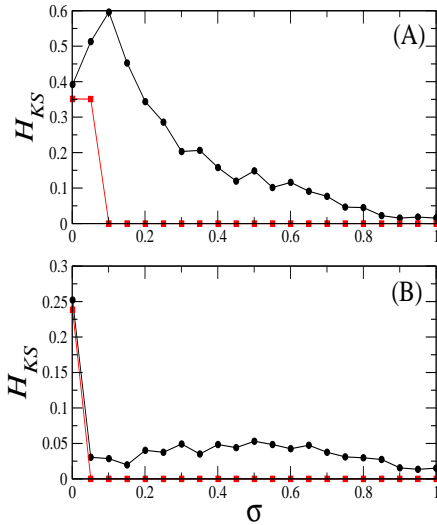


FIG. 9:  $H_{KS}$  for a network evolved by the method in Sec. XVIII, in circles, and in squares, for a network whose Laplacian is calculated by the method in Sec. XIX in order for the Laplacian to generate the same eigenvalues as the ones generated by the network Laplacian calculated by the evolution technique. In (A), we consider the same network topology whose connectivity is represented in Fig. 7(A), and in (B), we consider the same network topology whose connectivity is represented in Fig. 7(B). Note that in general, a Laplacian of an active network whose elements are connected with different coupling strengths, possess a smaller value of  $H_{KS}$ .

$\lambda^2$  becomes zero, simultaneously  $\lambda^1$  becomes also zero, a

consequence of the fact that all the neurons enter in a non-trivial but periodic oscillation. In general, however, both networks preserve the characteristics needed for optimal information transmission: large amounts of MIR and  $H_{KS}$ , however, the ones constructed by the evolution technique have larger  $H_{KS}$ , and possess a larger MIR for larger ranges of the coupling strength. The network obtained by the method in Sec. XIX is more synchronizable, a consequence of the fact that the coupling strengths are non-equal [18, 19].

## IX. ACTIVE NETWORKS FORMED BY NON-CHAOTIC ELEMENTS

The purpose of the present work is to describe how information is transmitted via an active media, a network formed by dynamical systems. There are three possible asymptotic stable behaviors for an autonomous dynamical system: chaotic, periodic, or quasi-periodic. A quasi-periodic behavior can be usually replaced by either a chaotic or a periodic one, by an arbitrary perturbation. For that reason, we neglect such a state and focus the attention on active channels that are either chaotic or periodic.

The purpose of the present section is dedicated to analyze how a source of information can be transmitted through active channels that are non-chaotic, that is periodic, and that possess negative Lyapunov exponents.

Equation (5) is defined for positive exponents. However, such an equation can also be used to calculate an upper bound for the rate of mutual information in systems that also possess negative Lyapunov exponents. Consider first a one-dimensional contracting system being perturbed by a random stimulus. Further consider that the stimulus changes the intrinsic dynamics of this system. This mimics the process under which an active element adapts to the presence of a stimulus.

Suppose the stimulus,  $\theta_n$ , can be described by a discrete binary random source with equal probabilities of generating '0' or '1'. Whenever  $\theta_n = 0$ , the system presents the dynamics  $x_{n+1} = x_n/2$ , otherwise  $x_{n+1} = (1 + x_n)/2$ . It is easy to see that the only Lyapunov exponent of this mapping,  $\lambda^1$ , which is equal to the conditional exponent,  $\lambda^1$ , is negative. Negative exponents do not contribute to the production of information. From Eq. (5) one would arrive at  $I_P=0$ . However, all the information about the stimulus is contained in the trajectory. If one measures the trajectory  $x_n$ , one knows exactly what the stimulus was, either a '0' or a '1'. The amount of information contained in the stimulus is  $\log(2)$  per iteration which equals the absolute value of the Lyapunov exponent,  $|\lambda^1|$ . In fact, it is easy to show that  $I_C = I_P = |\lambda^1| = |\lambda_1| = \log(2)$ , or if we use the interpretation of [21],  $I_C = I_P = \lambda$ , where  $\lambda = |\lambda_1|$  is the positive Lyapunov exponent of the time-inverse chaotic trajectory,  $x_{n+m}, x_{n+m-1}, \dots, x_0$ , which equals the rate of information production of the random source. So, in

this type of active communication channel, one would consider in Eq. (5) the positive Lyapunov exponents of the time-inverse trajectory, or the absolute value for the negative Lyapunov exponent.

Another example was given in [12]. In this reference we have shown that a chaotic stimulus perturbing an active system with a space contracting dynamics (a negative Lyapunov exponent) might produce a fractal set. We assume that one wants to obtain information about the stimulus by observing the fractal set. The rate of information retrieved about the stimulus on this fractal set equals the rate of information produced by the fractal set. This amount is given by  $D_1|\lambda|$ , where  $D_1$  is the information dimension of the fractal set and  $|\lambda|$  the absolute value of the negative Lyapunov exponent. In fact,  $D_1|\lambda|$  is also the rate of information produced by the stimulus. So, if an active system has a space contracting dynamics, the channel capacity equals the rate of information produced by the stimulus. In other words, the amount of information that the system allows to be transmitted equals the amount of information produced by the chaotic stimulus.

## X. THE ROLE OF A TIME-DEPENDENT STIMULUS IN AN ACTIVE NETWORK

The most general way of modeling the action of an arbitrary stimulus perturbing an active network is by stimulating it using uncorrelated white noise. Let us assume that we have a large network with all the channels operating in non-self-excitable fashion. We also assume that all the transversal eigenmodes of oscillations except one are stable, and therefore do not suffer the influence of the noise. Let us also assume that the noise is acting only on one structurally stable (= far from bifurcation points) element,  $S_k$ . To calculate the upper bound of the MIR between the element  $S_k$  and another element  $S_l$  in the network, we assume that the action of the noise does not alter the value of  $\lambda^1$ . Then, the noise on the element  $S_k$  is propagated along the vibrational mode associated with the one unstable transversal direction, whose conditional exponent is  $\lambda^2$ . As a consequence, the action of the noise might only increase  $\lambda^2$ , while not affecting the negativeness of all the other exponents ( $\lambda^m$ ,  $m > 2$ ), associated with stable transversal modes of oscillation. That means that the channels responsible for transmitting large amounts of information (associated with  $\lambda^m$ , with  $m$  large) will not be affected. So, for such types of noises, Eq. (5) of the autonomous network is an upper bound for the non-autonomous network.

Consider now a situation where the noise acts equally on all the elements of an active network. The mapping of Eq. (14) was proposed as a way to understand such a case. Consider the non-self-excitable map for  $s=-1$ . Note that the term  $\rho(x_n^2 + y_n^2)$  that enters equally in all the maps has statistical properties of a uniformly distributed random noise. Calculating  $I_P$  for  $\rho = 0$  (the

noise-free map) we arrive at  $I_P \cong 2\sigma$ , for small  $\sigma$ , while the true MIR  $I_C \cong 2(\sigma - \rho)$ . These results are confirmed by exact numerical calculation of the Lyapunov exponents of Eq. (14) as well as the calculation of the conditional exponents of the variational equations. So, this example suggests that Eq. (5) calculated for an autonomous non-perturbed network gives the upper bound for the mutual information rate in a non-autonomous network.

## XI. DISCUSSIONS

We have shown how to relate in an active network the rate of information that can be transmitted from one point to another, regarded as mutual information rate (MIR), the synchronization level among elements, and the connecting topology of the network. By active network, we mean a network formed by elements that have some intrinsic dynamics and can be described by classical dynamical systems, such as chaotic oscillators, neurons, phase oscillators, and so on.

Our main concern is to suggest how to construct an optimal network. A network that simultaneously transmits information at a large rate, is robust under couplings alterations, and further, it possesses a large number of independent channels of communication, pathways along which information travels.

We have studied two relevant conditions that the eigenvalues of the Laplacian matrix have to satisfy in order for one to have an optimal network. The Laplacian matrix describes the coupling strengths among each element in the active network.

The two eigenvalues conditions are designed in order to produce networks that are either self-excitable [maximizing Eq. (8)] or non-self-excitable [maximizing Eq. (9)] (see definition of self-excitability in Sec. XIV). Self-excitable networks have communication channels that transmit information in a higher rate for a large range of the coupling strength. Most of the oscillation modes in these networks are unstable, and therefore, information is mainly propagated in a desynchronous environment. Non-self-excitable networks have communication channels that transmit information in a higher rate for a small range of the coupling strength, however, they have channels that transmit reliable information in a moderate rate for large range of coupling strengths. Most of the oscillation modes in these networks are stable, and therefore, information is mainly propagated in a synchronous environment, a highly reliable environment for information transmission.

Therefore, to determine the topology of an optimal network one does not need to know information about the intrinsic dynamics of the elements forming the network.

Once the network topology is obtained such that the eigenvalues of the Laplacian matrix maximizes either the cost function in Eq. (8) or the one in Eq. (9), the actual amount of information that can be transmitted using the

obtained topology will depend on the intrinsic dynamics of the elements forming the network [ $F$  in Eq. (1)] and also on the type of coupling [ $H$  in Eq. (1)], of only two coupled elements [see Eq. (6)].

In the examples studied here, phase synchronization (PS) in the subspace  $(x, y)$  results in a great decrease of the KS-entropy (See Figs. 1 and 2) as well as of the MIR and  $I_P$ . However, a special type of partial phase synchronization, the BPS, appears simultaneously when some communication channel achieves its capacity. So, BPS [12] can provide an ideal environment for information transmission, probably a necessary requirement in the brain [22, 23]. Similarly, in networks of Rössler oscillators, a type of non-self-excitable network, PS is the phenomenon responsible to identify when the network is operating in a regime of high MIR [11, 24].

In order to construct an optimal network, we have used two approaches. One based on a Monte Carlo evolving technique, which randomly mutates the network topologies in order to maximize the cost functions in Eqs. (8) and (9) (see Sec. XVIII). We do not permit the existence of degenerate eigenvalues. As a consequence  $\gamma_N - \gamma_{N-1}$  as well as  $\gamma_3 - \gamma_2$  is never zero. The mutation is performed in order to maximize the cost function, but we only consider network topologies for which the value of the cost functions  $\mathcal{B}_1$  and  $\mathcal{B}_2$  remain constant for about 10,000 iterations of the evolving technique, within 1,000,000 iterations. Even though more mutations could lead to networks that have larger values of the cost function, we consider that a reasonably low number of mutations would recreate what usually happens in real networks. The other approach creates an arbitrary Laplacian which reproduces a desired set of eigenvalues.

Although both topologies provide larger amounts of MIR and  $H_{KS}$ , meaning large network and channel capacities, the topology provided by the evolution technique, which consider coupling strengths with equal strengths, is superior in what concerns information transmission. That agrees with the results of Ref. [12] which say that networks composed by elements with non-equal control parameters can transmit less information than networks formed by equal elements, since networks whose coupling strengths are non-equal can be considered to be a model for networks with non-equal control parameters.

So, if brain-networks somehow grow in order to maximize the amount of information transmission, simultaneously remaining very robust under coupling alterations, the minimal topology that small neural networks must have should be similar to the one in Fig. 7(A), i.e., a network with a star topology, presenting a central element, a hub, very well connected to other outer elements, which are sparsely connected.

Even though most of the examples worked out here concern simulations performed in a neural network of electrically coupled Hindmarsh-Rose neurons, our theoretical approaches to find optimal topologies can be used to a large class of dynamical systems, in particular also to networks of synaptically (chemically) connected neu-

rons. A neural network with neurons connected chemically would also be optimal if one connect neurons by maximizing either Eq. (8) or Eq. (9). The novelty introduced by the chemical synapses is that it can enhance (as compared with the electrical synapses) both the self-excitable (using excitable synapses) or the non-self-excitable (using inhibitory synapses) characteristic of the communication channels as well as it can enhance  $\langle I_P \rangle$  [25]. From the biological point-of-view, of course, the chemical synapses provide the long-range coupling between the neurons. So, the simulations performed here for the larger HR networks should be interpreted as to simulations of a general active network, since neurons connected electrically can only make nearest-neighbor connections.

## XII. METHODS

### XIII. CALCULATING THE MIR BY SYMBOLIC ENCODING THE TRAJECTORY

The MIR between two neurons can be roughly estimated by symbolizing the neurons trajectory and then measuring the mutual information from the Shannon entropy [27] of the symbolic sequences. From [27], the mutual information between two signals  $S_k$  and  $S_l$  is given by

$$I'_S = H(S_k) - H(S_l|S_k). \quad (10)$$

$H(S_k)$  is the uncertainty about what  $S_k$  has sent (entropy of the message), and  $H(S_l|S_k)$  is the uncertainty of what was sent, after observing  $S_l$ . In order to estimate the mutual information between two chaotic neurons by the symbolic ways, we have to proceed with a non-trivial technique to encode the trajectory, which constitutes a disadvantage of such technique to chaotic systems. We represent the time at which the  $n$ -th spike happens in  $S_k$  by  $T_k^n$ , and the time interval between the  $n$ -th and the  $(n+1)$ -th spikes, by  $\delta T_k^n$ . A spike happens when  $x_k$  becomes positive and we consider about 20000 spikes. We encode the spiking events using the following rule. The  $i$ -th symbol of the encoding is a “1” if a spike is found in the time interval  $[i\Delta, (i+1)\Delta[$ , and “0” otherwise. We choose  $\Delta \in [\min(\delta T_k^n), \max(\delta T_k^n)]$  in order to maximize  $I'_S$ . Each neuron produces a symbolic sequence that is split into small non-overlapping sequences of length  $L=12$ . The Shannon entropy of the encoding symbolic sequence (in units of bits), is estimated by  $\max H = -\sum_m P_m \log_2 P_m$  where  $P_m$  is the probability of finding one of the  $2^L$  possible symbolic sequences of length  $L$ . The term  $H(S_l|S_k)$  is calculated by  $H(S_l|S_k) = -H(S_l) + H(S_k; S_l)$ , with  $H(S_k; S_l)$  representing the Joint Entropy between both symbolic sequences for  $S_k$  and  $S_l$ .

Finally, the MIR (in units of bits/unit time),  $I_S$ , is

calculated from

$$I_S = \frac{I'_S}{\Delta \times L} \quad (11)$$

The calculation of the  $I_S$  by means of Eq. (11) should be expected to underestimate the real value for the MIR. Since the HR neurons have two time-scales, a large sequence of sequential zeros in the encoding symbolic sequence should be expected to be found between two bursts of spikes (large  $\delta T_k^n$  values), which lead to a reduction in the value of  $H(S_k)$  followed by an increase in the value of  $H(S_l|S_k)$ , since there will be a large sequence of zeros happening simultaneously in the encoding sequence for the interspike times of  $S_k$  and  $S_l$ .

#### XIV. SELF-EXCITABILITY

In Ref. [12] self-excitable was defined in the following way. An active network formed by  $N$  elements, is said to be self-excitable if  $H_{KS}(N, \sigma) > H_{KS}(N, \sigma = 0)$ , which means that the KS-entropy of the network increases as the coupling strength is increased. Thus, for non self-excitable systems, an increase in the coupling strength among the elements forming the network leads to a decrease in the KS-entropy of the network.

Here, we adopt also a more flexible definition, in terms of the properties of each communication channel. We define that a communication channel  $c^i$  behaves in a self-excitable fashion if  $\lambda^i > \lambda^1$ . It behaves in a non-self-excitable fashion if  $\lambda^i \leq \lambda^1$ .

#### XV. MUTUAL INFORMATION RATE (MIR), CHANNEL CAPACITY, AND NETWORK CAPACITY

In this work, the rate with which information is exchanged between two elements of the network is calculated by different ways. Using the approaches of Refs. [11, 12], we can have an estimate of the real value of the MIR, and we refer to this estimate as  $I_C$ . Whenever we use Eq. (5) to calculate the upper bound for the MIR, we will refer to it as  $I_P$ . Finally, whenever we calculate the MIR through the symbolic encoding of the trajectory as described in Sec. XIII, we refer to it as  $I_S$ .

We define the *channel capacity* of a communication channel formed by two oscillation modes depending on whether the channel behaves in a self-excitable fashion or not. So, for the studied network, every communication channel possess two channel capacities, the self-excitable capacity and the non-self-excitable one. A channel  $c^i$  operates with its self-excitable capacity when  $I_P^i$  is maximal, what happens at the parameter  $\sigma^{(i+1)*}$ . It operates with its non-self-excitable capacity when  $\lambda^{i+1} = 0$ .

We also define the channel capacity in an average sense. In that case, the averaged channel capacity is given by

the maximal value of the average value

$$\langle I_P \rangle = \sum_{i=2}^N \frac{1}{N-1} |\lambda^1 - \lambda^i|, \quad (12)$$

The *network capacity* of a network composed of  $N$  elements,  $\mathcal{C}_N(N)$ , is defined to be the maximum value of the Kolmogorov-Sinai (KS) entropy,  $H_{KS}$ , of the network. For chaotic networks, the KS-entropy, as shown by Pesin [28], is the sum of all the positive Lyapunov exponents. Notice that if  $I$  denotes the MIR then

$$I \leq H_{KS} \quad (13)$$

As shown in Ref. [12] and from the many examples treated here,  $\mathcal{C}_N(N) \propto N$ , and so, the network capacity grows linearly with the number of elements in an active network.

#### XVI. UNDERSTANDING EQ. (5)

Let us study Eq. (5) using an analytical example. For an introduction to the quantities shown here see Sec. XV. Consider the following two coupled maps:

$$\begin{aligned} x_{n+1} &= 2x_n - \rho x_n^2 + 2s\sigma(y_n - x_n), \\ y_{n+1} &= 2y_n - \rho y_n^2 + 2s\sigma(x_n - y_n), \end{aligned} \quad (14)$$

with  $\rho \geq 0$ ,  $s = \pm 1$ , and  $x_n, y_n \in [0, 1]$ , which can be accomplished by applying the *mod*(1) operation.

##### A. Positiveness of the MIR in Eq. (14)

Here, we assume that  $\rho=0$ . This map produces two Lyapunov exponents  $\lambda_1 = \log(2)$  and  $\lambda_2 = \log(2 - 4s\sigma)$ . Since this map is linear, the conditional exponents are equal to the Lyapunov exponents.

Using the same ideas of Ref. [12], actually an interpretation of the way Shannon [27] defines mutual information, the mutual information rate,  $I_P$ , exchanged between the variables  $x$  and  $y$  is given by the rate of information produced in the one-dimensional space of the variable  $x$ , denoted as  $H_x$ , plus the rate of information produced in the one-dimensional space of the variable  $y$ , denoted as  $H_y$ , minus the rate of information production in the  $(x, y)$  space, denoted as  $H_{xy}$ . But,  $H_x = H_y = \max(\lambda_1, \lambda_2)$ , and  $H_{xy} = H_{KS} = \lambda_1 + \lambda_2$ , if  $(\lambda_1, \lambda_2) > 0$ ,  $H_{xy} = H_{KS} = \lambda_1$ , if  $\lambda_2 < 0$ , and  $H_{xy} = H_{KS} = \lambda_2$ , otherwise.

So, either  $I_P = \lambda_1 - \lambda_2$ , case that happens for when  $s = +1$ , or  $I_P = \lambda_2 - \lambda_1$ , case that happens for when  $s = -1$ . If  $s = +1$ , the larger the coupling strength, the smaller the KS-entropy,  $H_{KS}$ . If  $s = -1$ , the larger the coupling strength, the larger  $H_{KS}$ . In fact, as we discuss further, Eq. (14) for  $s = -1$  is a model for a self-excitable channel, and for  $s = +1$  is a model for a non-self-excitable channel. In either case, the MIR can

be calculated by using the modulus operation as in  $I_P = |\lambda_1 - \lambda_2|$ . For larger networks, one can generalize such an equation using the conditional exponents arriving to an equation of the form as presented in Eq. (5).

This equation points out to a surprising fact. Even when the level of desynchronization in Eq. (14) is larger ( $\lambda^2 > \lambda^1$ ), which happens when  $s = -1$ , there is a positive amount of information being transferred between the two variables.

In Figure 10, we show the phase space of Eq. (14) for a coupling strength equal to  $\sigma=0.237$ . In (A), we illustrate a typical situation that happens in non-self-excitable channels ( $s = +1$ ). The elements become synchronous presenting a trajectory that most of the time lies on the synchronization manifold defined by  $x_n - y_n=0$ . In (B), we show a typical situation that happens in self-excitable channels ( $s = -1$ ). The elements become non-synchronous presenting a trajectory that lies on the transversal manifold defined by  $x_n + y_n - c=0$ , with  $c$  being a constant within the interval  $c \in [0, 1]$ .

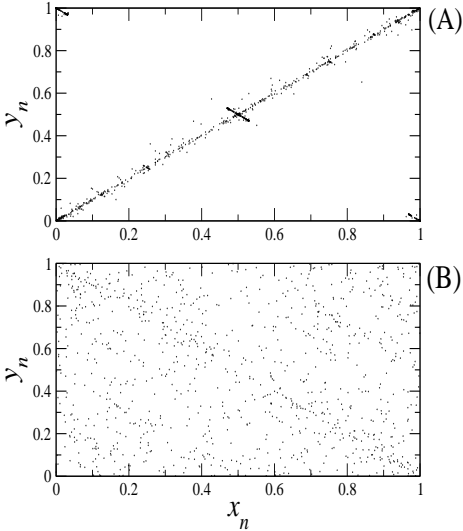


FIG. 10: Trajectory of Eq. (14) for  $\sigma=0.237$  with  $s = -1$  in (A) and  $s = 1$  in (B).

In (A), by observing the variable  $x_n$  one can correctly guess the value of  $y_n$  since  $x_n \cong y_n$ . Apparently, that is not the case in (B): by observing the variable  $x_n$ , one might have difficulty in guessing the value of the variable  $y_n$ , since  $c \in [0, 1]$ . Notice that the larger the amount of information being exchanged between  $x_n$  and  $y_n$ , the larger the chance that we guess correctly. In order to estimate the amount of information being exchanged between  $x_n$  and  $y_n$ , we proceed in the following way.

For the non-self-excitable channel ( $s=+1$ ), we coarse-grain the phase space in  $L^2$  small squares. Each square has one side that represents an interval of the domain of the variable  $x_n$  and another side which is an interval of the domain of the variable  $y_n$ . Calling  $p_x^{(i)}$ ,

the probability that a trajectory point visits the interval  $x_n = [(i-1)/L, i/L]$ , with  $i = 1, \dots, L$ , and  $p_y^{(i)}$ , the probability that a trajectory point visits the interval  $y_n = [(i-1)/L, i/L]$ , and finally,  $p_{x;y}^{(i,j)}$ , the probability that a trajectory point visits a square defined by  $x_n = [(i-1)/L, i/L]$ ,  $y_n = [(j-1)/L, j/L]$ , with  $j = 1, \dots, L$ , then, the MIR between  $x_n$  and  $y_n$ , denoted by  $I$ , is provided by

$$I = -1/\log(L) \left[ -\sum_i \log(p_x^{(i)}) - \sum_i \log(p_y^{(i)}) + \sum_{i,j} \log(p_{x;y}^{(i,j)}) \right]. \quad (15)$$

Notice that the evaluation of the MIR by Eq. (15) underestimates the real value for the MIR, since Eq. (14) is a dynamical system and the information produced by the dynamical variables (for example the term  $-\sum_i \log(p_x^{(i)})$  that measures the information produced by the variable  $x_n$ ) should be provided by conditional probabilities, i.e., the probability that a trajectory point has of visiting a given interval followed by another interval, and so on, in fact the assumption used to derive Eq. (5).

In Fig. 11(A), we show the phase space of Eq. (14) with  $s=+1$  and for  $\sigma = 0.237$ . In Fig. 11(B), we show by the plus symbol,  $I_P$ , as calculated by Eq. (5) and by circles,  $I$ , as estimated by Eq. (15).

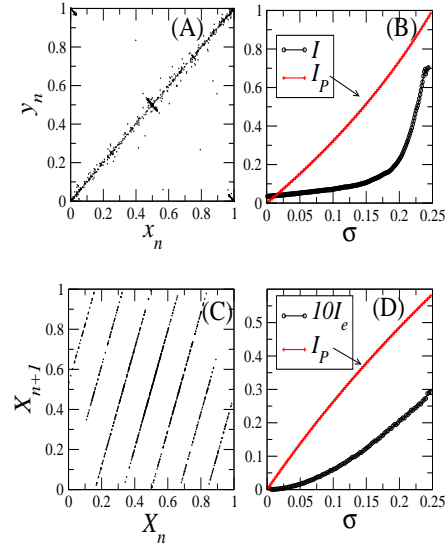


FIG. 11: Results for Eq. (14) with  $\sigma=0.237$  and  $s=-1$  [shown in (A) and (B)] and for  $s=+1$  [shown in (C) and (D)]. Phase space of Eq. (14) and in (B), the MIR as calculated by Eq. (5) and as estimated by Eq. (15). (C) Phase space of Eq. (14) in the new coordinate frame  $X_n$  vs.  $X_{n+1}$  and in (D), the MIR as calculated by Eq. (5) and as estimated by Eq. (16).

For the self-excitable channel ( $s=-1$ ) Eq. (15) supplies a null MIR, and therefore, it can no longer be used. But, as discussed in [12], the MIR can be coordinate dependent, and one desires to have the coordinate that maximizes the MIR. Aiming at maximizing the MIR,

when the channel is of the self-excitable type, we transform Eq. (14) into an appropriate coordinate system, along the transversal manifold, where most of the information about the trajectory position is located. We define the new coordinate as  $X_n = 1/2(x_n - y_n + 1)$  and  $X_{n+1} = 1/2(x_{n+1} - y_{n+1} + 1)$ . The trajectory  $(X_n, X_{n+1})$  in this new coordinate system [for the same parameters as in Fig. 10(B)] is depicted in Fig. 11(C).

The MIR being transferred between  $X_n$  and  $X_{n+1}$  is related to the knowledge we acquire about  $X_{n+1}$  by observing  $X_n$ , or vice-versa. In Fig. 11(C), we can only be certain about the value of  $X_{n+1}$ , when  $X_n$  is close to either 0 or 1.

To estimate the MIR, we recall that an encoded version of such a dynamical system can be treated as a symmetric binary channel of communication.  $X_n$  is regarded as the transmitter and  $X_{n+1}$  is regarded as the receiver. Whenever the map in the transformed coordinates  $X_n$  vs.  $X_{n+1}$  is non-invertible, we consider that by making measures of the trajectory point  $X_{n+1}$  one cannot guarantee the exact position of the trajectory of  $X_n$ , which constitutes an error in the transmission of information. Whenever the map is invertible, by measuring the trajectory of  $X_{n+1}$  one can surely know the exact position of the trajectory  $X_n$ , which corresponds to a correct transmission of information. Calling,  $p$  the probability at which the map is invertible, then, the MIR between  $X_n$  and  $X_{n+1}$  is given by

$$I_e = 1 + (1 - p) \log(1 - p) + p \log(p). \quad (16)$$

The value of  $10I_e$  for Eq. (14) with  $s = -1$  are shown in Fig. 11(D) by circles. The theoretical value,  $I_P$ , provided by Eq. (5) is shown by the plus symbol.

A final comment on the characteristics of a self-excitable channel and of a non-self-excitable channel is that while in a self-excitable channel the larger the synchronization level, the larger the MIR but the smaller the KS-entropy, in a non-self-excitable channel the larger the desynchronization level, the larger the MIR and the larger the KS-entropy. Note that  $H_{KS} = 2 \log(2) + \log(1 - 2s\sigma)$ , for  $\sigma < 0.25$ .

### B. Positiveness of the MIR for self-excitable channels in the (non-linear) HR network

To show that indeed  $I_P^i$  should be positive in case of a self-excitable channel in the HR network, one can imagine that in Eq. (1) the coupling strength is arbitrarily small and that  $N=2$ . At this situation, the Lyapunov exponent spectra obtained from Eq. (3) are a first-order perturbative version of the conditional exponents, and they appear organized by their strengths. One arrives at  $\lambda_1 \cong \lambda^2$  and  $\lambda_2 \cong \lambda^1$ , which means that the largest Lyapunov exponent equals the transversal conditional exponent and the second largest Lyapunov exponent equals the conditional exponent associated with the synchronous manifold, i.e., the Lyapunov exponent of Eq. (2). Using sim-

ilar arguments to the ones in Refs. [11, 12, 29], we have that the MIR is given by the largest Lyapunov exponent minus the second largest, and therefore,  $I_C = \lambda_1 - \lambda_2$ , which can be put in terms of conditional exponents as  $I_P \leq \lambda^2 - \lambda^1$ .

### C. The inequality in Eq. (5)

To explain the reason of the inequality in Eq. (5), consider the nonlinear term in Eq. (14) is non null and  $s=1$ , and proceeds as further.

For two coupled systems, the MIR can be written in terms of Lyapunov Exponents [12, 30]. For two coupled systems, the MIR can be exactly calculated by  $I_C = \lambda_1 - \lambda_2$ , since  $\lambda^{\parallel} = \lambda_1$  and  $\lambda^{\perp} = \lambda_2$ , assuming that both  $\lambda_1$  and  $\lambda_2$  are positive. Calculating the conditional exponents numerically, we can show that  $I_P \geq I_C$ , and thus  $I_P$  is an upper bound for the MIR. For more details on this inequality, see [31]

## XVII. BUST PHASE SYNCHRONIZATION (BPS)

Phase synchronization [32] is a phenomenon defined by

$$|\Delta\phi(k, l)| = |\phi_k - m\phi_l| \leq r, \quad (17)$$

where  $\phi_k$  and  $\phi_l$  are the phases of two elements  $S_k$  and  $S_l$ ,  $m = \omega_l/\omega_k$  is a real number [33], where  $\omega_k$  and  $\omega_l$  are the average frequencies of oscillation of the elements  $S_k$  and  $S_l$ , and  $r$  is a finite, real number [34]. In this work, we have used in Eq. (17)  $m = 1$ , which means that we search for  $\omega_k : \omega_l = 1:1$  (rational) phase synchronization [32]. If another type of  $\omega_k : \omega_l$ -PS is present, the methods in Refs. [34, 35, 36] can detect it.

The phase  $\phi$  is a function constructed on a 2D subspace, whose trajectory projection has proper rotation, i.e, it rotates around a well defined center of rotation. So, the phase is a function of a subspace. Usually, a good 2D subspace of the HR neurons is formed by the variables  $x$  and  $y$ , and whenever there is proper rotation in this subspace a phase can be calculated as shown in Ref. [37] by

$$\phi_s(t) = \int_0^t \frac{\dot{y}x - \dot{x}y}{(x^2 + y^2)} dt. \quad (18)$$

If there is no proper rotation in the subspace  $(x, y)$  one can still find proper rotation in the velocity subspace  $(\dot{x}, \dot{y})$  and a corresponding phase that measures the displacement of the tangent vector [35] can be calculated as shown in Ref. [37] by

$$\phi_v(t) = \int_0^t \frac{\ddot{y}\dot{x} - \ddot{x}\dot{y}}{(\dot{x}^2 + \dot{y}^2)} dt. \quad (19)$$

If a good 2D subspace can be found, one can also define a phase by means of Hilbert transform, which basically



transforms an oscillatory scalar signal into a two component signal [38]. In the active network of Eqs. (7) with an all-to-all topology and  $N=4$ , for the coupling strength interval  $\sigma \cong [0, 0.05]$ , the subspace  $(x, y)$  has proper rotation, and therefore,  $\phi_s(t)$  is well defined and can be calculated by Eq. (18). However, for this coupling interval, Eq. (17) is not satisfied, and therefore, there is no PS between any pair of neurons in the subspace  $(x, y)$ .

For the coupling strength interval  $\sigma \cong [0.05, 0.24]$ , the neurons trajectories lose proper rotation both in the subspaces  $(x, y)$  and  $(\dot{x}, \dot{y})$ . In such a case, neither  $\phi_s(t)$  nor  $\phi_v(t)$  can be calculated. This is due to the fact that the chaotic trajectory gets arbitrarily close to the neighborhood of the equilibrium point  $(x, y) = (0, 0)$ , a manifestation that a homoclinic orbit to this point exists.

In fact, the Hilbert transform fails to provide the phase from either scalar signals  $x$  or  $y$ , since these signals do not present any longer an oscillatory behavior close to the equilibrium point. In such cases, even the traditional technique to detect PS by defining the phase as a function that grows by  $2\pi$ , whenever a trajectory component crosses a threshold cannot be used. Since the trajectory comes arbitrarily close to the equilibrium point, no threshold can be defined such that the phase difference between pairs of neurons is bounded. Notice that by this definition the phase difference equals  $2\pi\Delta N$ , where  $\Delta N$  is the difference between the number of times the trajectory of  $S_k$  and  $S_l$  cross the threshold. For the neural networks,  $\Delta N$  could represent the difference between the number of spikes between two neurons. A spike is assumed to happen in  $S_k$  if  $x_k$  becomes positive.

In order to check if indeed PS exists in at least one subspace, alternative methods of detection must be employed as proposed in Refs. [35, 36]. In short, if PS exists in a subspace then by observing one neuron trajectory at the time the other bursts or spikes (or any typical event), there exists at least one special curve,  $\Gamma$ , in this subspace, for which the points obtained from these conditional observations do not visit its neighborhood. A curve  $\Gamma$  is defined in the following way. Given a point  $x_0$  in the attractor projected onto the subspace of one neuron where the phase is defined,  $\Gamma$  is the union of all points for which the phase, calculated from this initial point  $x_0$  reaches  $n\langle r \rangle$ , with  $n = 1, 2, 3, \dots, \infty$  and  $\langle r \rangle$  a constant, usually  $2\pi$ . Clearly an infinite number of curves  $\Gamma$  can be defined. For coupled systems with sufficiently close parameters that present in some subspace proper rotation, if the points obtained from the conditional observations do not visit the whole attractor projection on this subspace, one can always find a curve  $\Gamma$  that is far away from the conditional observations. Therefore, for such cases, to state the existence of PS one just has to check if the conditional observations are localized with respect to the attractor projection on the subspace where the phase is calculated.

Conditional observations of the neuron trajectory  $S_k$  in the subspace  $(x, y)$ , whenever another neuron  $S_l$  spikes, in the system modeled by Eqs. (7) with a star coupling

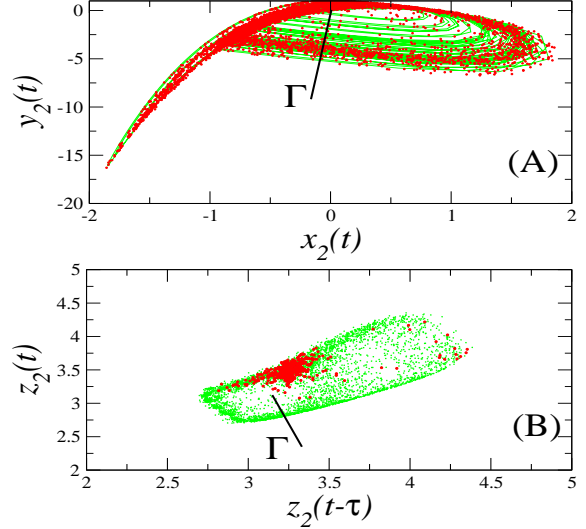


FIG. 12: The network of Eqs. (7) with a star configuration with  $N=4$ , and  $\sigma=0.265$ . The curve  $\Gamma$ , a continuous curve transversal to the trajectory, is pictorially represented by the straight line  $\Gamma$ . (A) the green line represents the attractor projection on the subspace  $(x, y)$  of the neuron  $S_2$ , and red circles represent the points obtained from the conditional observations of the neuron  $S_2$  whenever the neuron  $S_4$  spikes. The point  $(x, y) = (0, 0)$  does not belong to  $\Gamma$ . (B) Green dots represent the reconstructed attractor  $z_2(t) \times z_2(t - \tau)$ , for  $\tau=30$ , and red circles represent the points obtained from the conditional observation of neuron  $S_2$ , whenever the reconstructed trajectory of the neuron  $S_4$  crosses the threshold line  $z_4(t - \tau) = 3.25$  and  $z_4(t) > 3$ .

topology and  $N=4$ , are not localized with respect to a curve  $\Gamma$ , for the coupling strength  $\sigma < \sigma_{PS}$ . An example can be seen in Fig. 12(A), for  $\sigma = 0.265$ . The set of points produced by the conditional observations are represented by red circles, and the attractor by the green points. Therefore, there is no PS in the subspace  $(x, y)$ .

In order to know on which subspace PS occurs, we proceed in the following way. We reconstruct the neuron attractors by means of the time-delay technique, using the variable  $z$ . This variable describes the slow time-scale, responsible for the occurrence of bursts. The reconstructed attractor  $z(t) \times z(t - \tau)$  has proper rotation [see Fig. 12(B)] and the points obtained from the conditional observations do not visit the neighborhood of a curve  $\Gamma$ , then, there is PS in this subspace. Indeed, we find localized sets with respect to a curve  $\Gamma$  in the reconstructed subspace  $(z(t) \times z(t - \tau))$ , for  $\sigma \geq 0.265$ . So,  $\sigma_{BPS}=0.265$ .

So, for the coupling  $\sigma = [\sigma_{BPS}, \sigma_{PS}]$ , there is no PS in the subspace  $(x, y)$  but there is PS in the subspace of the variable  $z$ . In this type of synchronous behavior, the bursts are phase synchronized while the spikes are not. This behavior is regarded as bursting phase synchronization (BPS). For simplicity in the analyses, we say that

BPS happens when for at least one pair of neurons there is phase synchronization in the bursts. Phase synchronization (PS) happens in the network when the average absolute phase difference

$$\frac{2}{N(N-1)} \sum_k \sum_l |\Delta\phi_L(k,l)|,$$

with  $k = 1, N-1$  and  $l = k+1, N$  among all the pairs of elements, is smaller than  $2\pi$ , with the phases defined by either Eq. (18) or Eq. (19), where the index  $L$  represents either the index  $s$  or  $v$ . Further, we say complete synchronization (CS) takes place [17], when the variables of one neuron equal the variables of all the other neurons.

For the analyses in this work,  $\sigma_{BPS}$  represents the coupling parameter for which BPS first appears, i.e., BPS exists if  $\sigma \geq \sigma_{BPS}$ .  $\sigma_{PS}$  represents the coupling parameter for which PS first appears, i.e., PS exists if  $\sigma \geq \sigma_{PS}$ . Finally,  $\sigma_{CS}$  represents the coupling parameter for which CS first appears, i.e., CS exists if  $\sigma \geq \sigma_{CS}$ . There might exist particular parameters for which PS (or BPS) is lost even if  $\sigma \geq \sigma_{PS}$  (resp.  $\sigma \geq \sigma_{BPS}$ ). But these parameters are not typical and we will ignore them. For example, in the network composed by 6 elements with the nearest-neighbor topology [Fig. 2(B)], for  $\sigma \cong 0.825$  PS is lost.

Note that these phenomena happen in a hierarchical way organized by the "intensity" of synchronization. The presence of a stronger type of synchronization implies in the presence of other softer types of synchronization in the following order: CS  $\rightarrow$  PS  $\rightarrow$  BPS.

### XVIII. EVOLUTIONARY CONSTRUCTION OF A NETWORK

In our simulations, we have evolved networks of equal bidirectional couplings [39]. That means that the Laplacian in Eq. (1) is a symmetric matrix of dimension  $N$  with integer entries  $\{0, 1\}$  for the off diagonal elements, and the diagonal elements equal to  $-\sum_j \mathcal{G}_{ij}$ , with  $i \neq j$ .

Finding the network topologies which maximize  $\mathcal{B}$  in Eq. (8) is impractical even for moderately large  $N$ . Figuring out by "brute force" which Laplacian produces the desired eigenvalue spectra would require the inspection of a number of  $\frac{2^{N(N-1)/2}}{N!}$  configurations. To overcome this difficulty, Ref. [14] proposed an evolutionary procedure in order to reconstruct the network in order to maximize some cost function. Their procedure has two main steps regarded as *mutation* and *selection*. The mutation steps correspond to a random modification of the pattern of connections. The selection steps consist in accepting or rejecting the mutated network, in accordance with the criterion of maximization of the cost function  $\mathcal{B}$ , in Eq. (8).

We consider a random initial network configuration, with  $N$  elements, which produce an initial Laplacian  $\mathcal{G}_0$ , whose eigenvalues produce a value  $\mathcal{B}_0$  for the cost function. We take at random one element of this network

and delete all links connected to it. In the following, we choose randomly a new degree  $k$  to this element and connect this element (in a bidirectional way) to  $k$  other elements randomly chosen. This procedure generates a new network that possesses the Laplacian  $\mathcal{G}'$ , whose eigenvalues produce a value  $\mathcal{B}'$ . To decide if this mutation is accepted or not, we calculate  $\Delta\epsilon = \mathcal{B}' - \mathcal{B}_0$ . If  $\Delta\epsilon > 0$ , the new network whose Laplacian is  $\mathcal{G}'$  is accepted. If, on the other hand,  $\Delta\epsilon < 0$ , we still accept the new mutation, but with a probability  $p(\Delta\epsilon) = \exp(-\Delta\epsilon/T)$ . If a mutation is accepted then the network whose Laplacian is  $\mathcal{G}_0$  is replaced by the network whose Laplacian is  $\mathcal{G}'$ .

The parameter  $T$  is a kind of "temperature" which controls the level of noise responsible for the mutations. It controls whether the evolution process converges or not. Usually, for high temperatures one expects the evolution never to converge, since new mutations that maximizes  $\mathcal{B}$  are often not accepted. In our simulations, we have used  $T \cong 0.0005$ .

These steps are applied iteratively up to the point when  $|\Delta\epsilon| = 0$  for about 10,000 steps, being that we consider an evolution time of the order of 1,000,000 steps. That means that the evolution process has converged after the elapse of some time to an equilibrium state. If for more than one network topology  $|\Delta\epsilon| = 0$  for about 10,000 steps, we choose the network that has the larger  $\mathcal{B}$  value.

This constraint avoids the task of finding the most optimal network topology. However, we consider that a reasonably low number of mutations would recreate what usually happens in real networks.

### XIX. CONSTRUCTING A NETWORK FROM A SET OF EIGENVALUES

Given a  $N \times N$  Laplacian matrix  $\mathcal{G}$ , we can diagonalize it by an orthogonal transformation, viz

$$\mathbf{O}^T \mathcal{G} \mathbf{O} = \gamma \mathbf{1}, \quad (20)$$

where  $\mathbf{1}$  represents the Unity matrix,  $\gamma$  represents the vector that contains the set of eigenvalues  $\gamma_i$  of  $\mathcal{G}$  ( $i = 1, \dots, N$ ), and  $\mathbf{O}$  is an orthogonal matrix,  $\mathbf{O} \mathbf{O}^T = \mathbf{O}^T \mathbf{O} = \mathbf{1}$ , whose columns are constructed with the orthogonal eigenvectors of  $\mathcal{G}$ , namely  $\mathbf{O} = [\vec{v}_1, \vec{v}_2, \dots, \vec{v}_N]$ . Accordingly,

$$\mathcal{G} = \mathbf{O} \cdot \gamma \mathbf{1} \mathbf{O}^T, \quad (21)$$

which means that  $\mathcal{G}$  can be decomposed into a multiplication of orthogonal matrices. By using the spectral form of Eq. (21), the Laplacian  $\mathcal{G}$  can be calculated from

$$\mathcal{G} = \sum_{i=1}^N \vec{v}_i \cdot \gamma_i \cdot \vec{v}_i^T. \quad (22)$$

Any other Laplacian,  $\mathcal{G}'$ , can be constructed by using

the set of eigenvalues  $\gamma$ , viz

$$\mathcal{G}' = \sum_{i=1}^N \vec{v}_i' \cdot \gamma_i \cdot \vec{v}_i'^T. \quad (23)$$

Of course, in order for the active network that is constructed using  $\mathcal{G}'$  to present the synchronization manifold  $x_1 = x_2 = x_3 = \dots = x_n$ , the vector  $\vec{v}_1'$ , with  $N$  elements, is given by  $\vec{v}_1'^T = \frac{1}{\sqrt{N}}[1, 1, 1, \dots, 1]$ , and the other vectors are found by choosing arbitrary vectors  $\vec{v}_i'$  which are made orthogonal using the Gram-Schmidt technique.

**Acknowledgment** We thank C. Trallero who has promptly so many times discussed with MSB related topics to this work. MSB thanks a stay at the International Centre for Theoretical Physics (ICTP), where he had the great opportunity to meet and discuss some of

the ideas presented in this work with H. Cerdeira and R. Ramaswamy. MSB also thanks K. Josić for having asked what would happen if the transversal conditional Lyapunovs were larger than the one associated with the synchronization manifold and T. Nishikawa for having asked what would happen if  $s$  in Eq. (14) is positive, two questions whose answer can be seen in Appendix XVI. Finally, we would like to express our gratitude to L. Pecora, for clarifying the use of the Spectral Theorem in the construction of a Laplacian matrix with a given set of eigenvalues and for insisting in presenting a more rigorous argument concerning the calculation of the conditional exponents. This work is supported in part by the CNPq and FAPESP. MSH is the Martin Gutzwiller Fellow 2007/2008.

- 
- [1] Hindmarsh JL and Rose RM (1984) A model of neuronal bursting using three coupled first order differential equations. *Proc. R. Soc. Lond. B*, 221: 87-102.
- [2] Smith VA, Yu J, Smulders, TV, Hartemink AJ, Jarvis ED (2006) Computation inference of neural information flow networks. *PLoS Comput Bio* 2: e161.
- [3] Eggermont JJ (1998) Is there a Neural Code. *Neuroscience & Biobehavioral Reviews* 22: 355-370.
- [4] Borst A and Theunissen FE (1999) Information theory and neural coding. *Nature neuroscience* 2: 947-957.
- [5] Strong SP, Köberle R, de Ruyter van Steveninck RR, and Bialek W (1998) Entropy and Information in Neural Spike Trains. *Phys. Rev. Lett.* 80: 197-201.
- [6] Palus M, Komárek V, Procházka T, Hrnčíř Z, Sterbová K (2001) Synchronization and information flow in EEGs of Epileptic Patients *IEEE Engineering in medicine and biology*. September/October: 65-71.
- [7] Żochowski M and Dzakpasu (2004) R Conditional entropies, phase synchronization and changes in the directionality of information flow in neural systems *J. Phys. A: Math. Gen.* 37: 3823-3834.
- [8] Jirsa VK (2004) Connectivity and Dynamics of Neural Information Processing. *Neuroinformatics* 2: 1-22.
- [9] Schreiber T (2000) Measuring Information Transfer *Phys. Rev. Lett.* 85: 461-464.
- [10] San Liang X and Kleeman R (2005) Information transfer between dynamical systems components. *Phys. Rev. Lett.* 95: 244101-1- 244101-4.
- [11] Baptista MS and Kurths J (2005) Chaotic channel. *Phys. Rev. E* 72: 045202R.
- [12] Baptista MS and Kurths J (2007) Transmission of information in active networks, to appear in *Phys. Rev. E*.
- [13] der Malsburg CV, Nervous structures with dynamical links. (1985) *Ber. Bunsenges Phys. Chem.* 89: 703-710.
- [14] Ipsen M and Mikhailov AS Evolutionary reconstruction of networks (2002) *Phys. Rev. E* 66: 046109.
- [15] Pareti G and Palma A (2004) Does the brain oscillate? The dispute on neuronal synchronization. *Neurol. Sci.* 25: 41-47.
- [16] Many pathological brain diseases, as Epilepsy, are associated with the appearance of synchronization.
- [17] Heagy JF, Carrol TL, and Pecora LM (1994) Synchronous chaos in coupled oscillators systems *Phys. Rev. E* 50: 1874-1885; Heagy JF, Carrol TL, and Pecora LM (1995) Short Wavelength bifurcations and size instabilities in coupled oscillator systems. *Phys. Rev. Lett.* 74: 4185-4188; Pecora LM and Carroll (1998) Master stability functions for synchronized coupled systems. *Phys. Rev. Lett.* 80: 2109-2112; Pecora LM (1998) Synchronization conditions and desynchronization patterns in coupled limit-cycle and chaotic systems. *Phys. Rev. E* 58: 347-360; Barahona M and Pecora LM (2002) Synchronization in small-world systems. *Phys. Rev. Lett.* 89: 054101.
- [18] Chavez M, Hwang DU, Martinerie J, Boccaletti S (2006) Degree mixing and the enhancement of synchronization in complex weighted networks, *Phys. Rev. E* 74: 066107; Chavez M, Hwang DU, Amann A, *et al.* (2006) Synchronizing weighted complex networks *CHAOS* 16: 015106; Chavez M, Hwang DU, Amann A, *et al.* Synchronization is enhanced in weighted complex networks (2005) *Phys. Rev. Lett.* 94: 218701.
- [19] Zhou CS, Kurths J (2006) Dynamical weights and enhanced synchronization in adaptive complex networks *Phys. Rev. Lett.* 96: 164102; Zhou CS, Motter AE, Kurths J Universality in the synchronization of weighted random networks (2006) *Phys. Rev. Lett.* 96: 034101.
- [20] Djurfeldt M, Lundqvist M, Johansson C, *et al.*, Project report for Blue Gene Watson Consortium Days: Massively parallel simulation of brain-scale neuronal networks models (Stockholm University, Sweden 2006).
- [21] Corron NJ, Hayes ST, Pethel SD, *et al.* (2006) Chaos without Nonlinear Dynamics. *Phys. Rev. Lett.* 97: 024101.
- [22] Lachaux JP, Rodriguez E, Martinerie J, and Varela FJ (1999) Measuring Phase Synchrony in Brain Signals. *Human Brain Mapping* 8: 194-208.
- [23] Tass PA, Fieseler T, Dammers J, *et al.* (2003) Synchronization Tomography: A method for three-dimensional localization of phase synchronized neuronal population in

- the Human brain using magnetoencephalography. Phys. Rev. Lett. 90: 0881011 (2003).
- [24] Baptista MS, Zhou C, and Kurths J (2006) Information transmission in phase synchronous chaotic arrays. Chinese Phys. Lett. 23: 560-564.
- [25] Moukam Kakmeni FM and Baptista MS, "Information and synchronization in Hindmarsch-Rose neural networks of neurons chemically and electrically connected.", manuscript in preparation.
- [26] Mandsman AS and Schwartz AS, (2007) Complete chaotic synchronization in mutually coupled time-delay systems. Phys. Rev. E 75: 026201.
- [27] Shannon CE and Weaver W, *The Mathematical Theory of Communication* (The University of Illinois Press, 1949).
- [28] Pesin YB (1977) Characteristic Lyapunov Exponents and Smooth Ergodic Theory. Russian Math. Surveys 32: 55-114.
- [29] Baptista MS, Garcia SP, Dana S, and Kurths J, "Transmission of information in active networks: an experimental point of view", to appear in Europhysics Journal.
- [30] Mendes RV (1998) Conditional exponents, entropies and a measure of dynamical self-organization. Phys. Lett. A 248: 167-171; (2000) Characterizing self-organization and coevolution by ergodic invariants. Physica A 276: 550-571.
- [31] M. S. Baptista, F. Moukam Kakmeni, Gian Luigi del Magno, M. S. Hussein. "Bounds for the Kolmogorov-Sinai entropy of active networks in terms of conditional Lyapunov exponents", to be subm. for publication.
- [32] Pikovsky A, Rosenblum M, and Kurths J, *Synchronization A Universal Concept in Nonlinear Sciences* (Cambridge, London 2003).
- [33] Baptista MS, Boccaletti S, Josić K, and Leyva I (2004) Irrational phase synchronization. Phys. Rev. E 69: 056228.
- [34] Baptista MS, Pereira T, and Kurths J (2006) Upper bounds in phase synchronous weak-coherent chaotic attractors. Physica D 216: 260-268.
- [35] Baptista MS, Pereira T, Sartorelli JC, *et al.* (2005) Non-transitive maps in phase synchronization. Physica D 212: 216-232.
- [36] Pereira T, Baptista MS, and Kurths J (2007) General framework for phase synchronization through localized maps. Phys. Rev. E 75: 026216.
- [37] Pereira T., Baptista MS, and Kurths J (2007) Average period and phase of chaotic oscillators. Phys. Lett. A 362: 159-165.
- [38] Gabor D Theory of Communication (1946) J. IEE London 93: 429-457.
- [39] Systems of bidirectional equal couplings can be considered as models of electrical gap junctions, a coupling that allows bidirectional flowing of information in neural networks.